Corrosion Analysis & Preventive Measures Against H_2S in Regeneration Gas Heating & Cooling System

By

Muhammad Zeshan Rafiq

School of Chemical and Materials Engineering

National University of Sciences and Technology

2023

Corrosion Analysis & Preventive Measures Against H_2S in Regeneration Gas Heating & Cooling System

Name: Muhammad Zeshan Rafiq

Reg. No: 00000317521

This thesis is submitted as a partial fulfillment of the requirements for the degree of

MS (Materials and Surface Engineering)

Supervisor Name: Dr. Muhammad Shahid

School of Chemical and Materials Engineering (SCME)

National University of Sciences and Technology (NUST)

H-12 Islamabad, Pakistan

July 2023

THESIS ACCEPTANCE CERTIFICATE

Certified that final copy of MS thesis written by Mr **Muhammad Zeshan Rafiq** (Registration No 00000317521), of School of Chemical & Materials Engineering (SCME) has been vetted by undersigned, found complete in all respects as per NUST Statues/Regulations, is free of plagiarism, errors, and mistakes and is accepted as partial fulfillment for award of MS degree. It is further certified that necessary amendments as pointed out by GEC members of the scholar have also been incorporated in the said thesis.

Signature: ____________________

Name of Supervisor: **Dr Muhammad Shahid**

Date: 14-9-23

Signature (HOD): ____________________

Date: 14/9/23

Signature (Dean/Principal): ____________________

Date: 14-9-2023

FORM TH-1

National University of Sciences & Technology

MASTER'S THESIS WORK

Formulation of Guidance and Examination Committee

Name: **Muhammad Zeshan Rafiq** NUST Regn No: **00000317521**
Department: **School of Chemical & Materials Engineering** Specialization: **Material & surface Engineering**

Credit Hour Completed: 21 24 CGPA: 3.21 3.25

Course Work Completed

S/No	Code	Title	Core/Elective	CH	Grade
1	MSE 811	Materials Thermodynamics	Core	3.0	B
2	MSE 821	Mechanical Behavior of Materials	Core	3.0	C+
3	MSE 882	Corrosion and Control Engineering	Elective	3.0	C+
4	MSE 812	Phase Transformation & Microstructures	Core	3.0	A
5	MSE 851	Surface Engineering & Characterization	Core	3.0	B+
6	MSE 861	Engineering Ceramics and Glasses	Elective	3.0	B+
7	MSE 881	Manufacturing Processes	Elective	3.0	B+
8	RM-898	Research methodology	Add	2	Q
9	MSE-854	Characterization of materials	Elective	3	B+

Date: 28.06.21 Student's Signature: ____________

Thesis Committee Members:

Supervisors Name: **Dr. Malik Adeel Umer** Signature: ____________

Members:

1. Name: **Dr. Aftab Akram**
   Department: **SCME** Signature: ____________
2. Name: **Dr. Farhan Javaid**
   Department: **SCME** Signature: ____________
3. Name: ____________
   Department: ______ Signature: ____________

Date: 28/6/2021 ____________
Signature of Head of Department

APPROVAL
Dean / Principal

____
Date: 2-8-2021

Distribution

- 1 x copy to Exam Branch, HQ NUST
- 1 x copy to PGP Dte, HQ NUST
- 1 x copy to Exam Branch, Respective Institute

FORM TH-4

National University of Sciences &Technology (NUST)

MASTER'S THESIS WORK

We hereby recommend that the dissertation prepared under our supervision by

Regn No & Name: **00000317521 Muhammad Zeshan Rafiq**

Title: **Corrosion Analysis & Preventive Measures Against H_2S in Regeneration Heating & Cooling System.**

Presented on: **16 Aug 2023** at: **1430 hrs in SCME Seminar Hall**

Be accepted in partial fulfillment of the requirements for the award of Masters of Science degree in **Materials & Surface Engineering**.

Guidance & Examination Committee Members

Name: **Dr Farhan Javaid** Signature:

Name: **Dr Muhammad Aftab Akram** Signature:

Supervisor's Name: **Dr Muhammad Shahid** Signature:

Dated: 16-8-23

Head of Department

Date 21/8/23

Dean/Principal

Date 21.8-2023

School of Chemical &Materials Engineering (SCME)

Dedication

Dedicated to my exceptional parents and adored Wife (Sahar Akbar) whose tremendous support and cooperation led me to this wonderful accomplishment.

Acknowledgment

First and foremost, I would like to thank Allah Almighty for giving me the strength and opportunity to undertake this research study and to preserve and complete it satisfactorily. Without His blessings, this work would not have been possible.

I wish to express my sincere gratitude to my supervisor, Dr Muhammad Shahid, who has been a tremendous mentor for me. I would like to thank him for his encouragement, enthusiastic supervision, and help during my research and for allowing me to grow as a research scientist. I am also grateful to lab fellows and seniors for their support.

Finally, I would like to thank my family and friends for their unconditional support and encouragement. To the most important people in my life, my parents, my siblings, this research work could only be completed with your support foremost.

Muhammad Zeeshan Rafiq

Reg No. 00000317521

Abstract

Regeneration gas cooling and heating system installed in oil and gas processing plant plays a crucial role in removal of carbon dioxide (CO_2) and hydrogen sulfide (H_2S), from natural gas streams. The commingled flow of gases received from different wells in oil and gas exploration contains H_2S, which poses a risk to the regeneration heating and cooling system. Analysis of hydrogen sulfide (H_2S) corrosion and prevention measures is essentially required in the regeneration gas cooling and heating system including the feed and return lines.

To evaluate the structural strength and susceptibility to H_2S corrosion in regeneration gas heating and cooling system, a combination of conventional and advanced non-destructive testing methods is used. Non-destructive testing reports are analyzed according to internationally recognized codes and standards such as API-510 and ASME Sec VIII DIV 1.These assessments determine corrosion rates, remaining lifespan of the equipment, minimum thickness requirements, and maximum operating pressure. Recommendations are provided for the mitigation of H_2S corrosion, including the selection of chemical treatments such as H_2S scavengers and inhibition programs, pH control chemicals, installation of corrosion monitoring tools and post-weld heat treatments.

Stress corrosion cracking (SSC) is a type of damage that occurs when certain metals are exposed to stress, corrosion, water, and hydrogen sulfide (H_2S). To prevent SSC in several types of steels, it is important to use a process called post-weld heat treatment (PWHT). PWHT reduces hardness and stress in the metal, which helps lower the risk of SSC. Certain welding techniques can also increase the chance of SSC because of heat affected zone (HAZ).

The results of this research align closely with published data and offer an effective procedure for analysis of H_2S corrosion in the regeneration gas cooling and heating system and provides preventive measures against anticipated H_2S damage mechanism. The proposed procedure is a significant improvement in addressing H_2S corrosion problems and provides a more realistic solution for industrial applications to reduce downtime, production loss and loss of human life.

Table of Contents

1. Introduction 1
1.1 Background, Scope, and Motivation: 2
1.2 Types of Heat Exchangers Failures: 4
1.3 Failure mechanisms: 4
1.3.1 Mechanical Failure: 5
1.3.2 Metal Erosion: 6
1.3.3 Flow Velocity Effect: 7
1.3.4 Vibration: 7
1.4 Galvanic Effect: 8
1.5 Thermal fatigue: 8
1.6 Chemical Induced Corrosion: 9
1.7 Fouling and corrosion: 11
1.8 Mesa Corrosion: 13
1.9 Pitting Corrosion: 13
1.10 Sources of hydrogen sulfide: 15
1.11 H_2S Corrosion: 16
1.11.1 Impact of pH on H_2S corrosion: 39
1.11.2 Impact of Partial Pressure & Concentration on H_2S Corrosion: 39
1.11.3 Impact of Temperature: 39
1.11.4 Sweet spot: 40
1.11.5 Impact of Hardness of H_2S Corrosion: 40
1.11.6 Increased susceptibility to corrosion: 40
1.11.7 Stress corrosion cracking (SCC): 40
1.11.8 Hardness-induced cracking: 40
1.11.9 Impact of H_2S to Human life and Equipment: 41
1.12 Analysis of H_2S in the regenerator gas cooling and heating system: 18
1.13 Conventional & advanced NDT techniques: 19
1.13.1 Using Remote Field Eddy Current Testing to Detect Stress Corrosion Cracks in Gas Transmission Pipelines: 19

1.13.2 Ultrasonic flaw detection: 20
1.13.3 Ultrasonic thickness gauging: 22
1.13.4 Magnetic particle inspection: 22
1.13.5 Eddy current testing and Remote field testing: 23
1.13.6 Metallography by Portable microscope techniques: 23
2 Literature Review 25
2.1 Analysis & Investigation of Failures in regeneration gas heating and cooling system: 26
2.2 Investigating the Influence of H_2S/CO_2 Partial Pressure Ratio on the Tensile Properties of X80 Pipeline Steel: 28
2.3 Failure Analysis of Type 304 Stainless Steel Amine Exchanger Sheets in a Gas Sweetening Plant: 28
2.4 H_2S challenges presented to ESP systems: 29
2.5 Inspecting Mechanical Properties and Corrosion Behavior of Rubber Packer in CO_2-H_2S Gas Wells: 29
2.6 Investigation on the H_2S-Resistant behaviors of acicular Ferrite and ultrafine Ferrite: 31
2.7 Effect of H_2S interaction with pre-strain on the mechanical properties of High-Strength X80 Steel: 32
2.8 Electrochemical & SSCC behavior of tubing steels in H_2S/CO_2 annular environment: 32
2.9 Investigation of pH_2S influence on 3% Cr Tubing steel corrosion behaviors in CO_2-H_2S-Cl_2 environment: 33
2.10 Role of microstructure on the sulfide stress cracking of Oil and gas pipeline steels: 34
2.11 Investigating the impact of heat treatment and microstructural transformations on API X-65 pipeline steel's susceptibility to HIC and corrosion in an H_2S environment: 35
2.12 Assessment of SSC in AISI 316L Stainless Steel under H_2S Environment during Service: 36
2.13 Risk Assessment of Corrosion Under Insulation (CUI) on Industrial Piping: .. 37

2.14 International codes and standards for H_2S corrosion analysis: 38
2.14.1 National Association of corrosion Engineers (NACE): 38
2.14.2 American Petroleum Institute (API): 38
2.14.3 American society for testing of materials ASTM International:................ 38
3 Experimental Work 42
3.1 Methodology: 42
3.2 Internal Inspection: 43
3.3 Visual inspection: 43
3.4 Eddy current testing / Remote field testing (RFT): 44
3.5 Dye Penetrant Inspection: 45
3.5.1 Surface Preparation for Dye penetration: 46
3.5.2 Clean the surface: 46
3.5.3 Dry the surface: 46
3.5.4 Surface Roughness: 46
3.5.5 Application of dye: 46
3.5.6 Removal of excess dye: 46
3.5.7 Application of developer: 46
3.5.8 Inspection of the surface for defects: 47
3.6 Magnetic particle inspection: 47
3.6.1 Surface Preparation for Magnetic particle inspection: 47
3.6.2 Identification of suspected defects: 48
3.6.3 Pre-cleaning of Surface: 48
3.6.4 Magnetization of surface: 48
3.6.5 Inspection of Surface: 48
3.6.6 Post-inspection cleaning: 48
3.7 Ultrasonic flaw detection: 48
3.7.1 Ultrasonic flaw detection setup: 49
3.7.2 Selection of Couplant: 49
3.7.3 Adjustment of instrument: 49
3.7.4 Scanning of the weld joints: 49
3.8 Ultrasonic thickness gauging: 50

3.8.1 Selection of Thickness / condition monitoring location: 50
3.8.2 Calibration of Thickness meter: 51
3.8.3 Selection of Couplant: 51
3.8.4 Placement of Thickness meter probe: 51
3.8.5 Measurement of thickness: 51
3.9 Hardness testing: 52
3.9.1 Sample Preparation: 52
3.9.2 Calibration and setup of Hardness tester: 52
3.9.3 Placement of Hardness tester: 52
3.10 In-Situ Metallography: 53
3.10.1 Sample selection: 53
3.10.2 Sample Preparation: 53
3.10.3 Microscopic examination by portable Microscope: 54
3.11 Overall inspection pictorial display: 55
Chapter 4: 57
4 Results & Discussions 57
4.1 Visual inspection : 57
4.2 Remote Field Testing of tubes: 58
4.3 Dye Penetrant Inspection: 60
4.4 Magnetic particle inspection: 61
4.5 Ultrasonic flaw examination: 62
4.6 UT Gauging: 63
4.7 Ultrasonic thickness gauging: 63
4.8 Hardness Testing: 65
4.9 IN-situ metallography: 67
4.10 Produced water Analysis Report: 69
4.11 Inspection finding summary: 70
4.11.1 Formulas for Key Parameter Calculations : 70
4.11.2 Calculation of Key Parameters: 71
5 Conclusions 73
6 Recommendation against H_2S corrosion mitigations: 75

APPENDIX- I 76
APPENDIX- II 77
References 78

List of figures

Figure 1. General Corrosion mechanism 5
Figure 2. (a) Metal Erosion & (b) Erosion corrosion (c) Accelerated corrosion 6
Figure 3. Noise & vibration in fluid pipe 7
Figure 4. Vibration induced split. 8
Figure 5. Galvanic Corrosion 8
Figure 6. Thermal Fatigue 9
Figure 7. (a) X-section of tubing damage via pitting (b) Uniform corrosion 10
Figure 8. (a) Intergranular corrosion (b) Crevice corrosion under gasket of plate heat exchanger 11
Figure 9. Fouling process 12
Figure 10. Mesa corrosion sharp edges holes 13
Figure 11. (a) Narrow, deep pit (b) Shallow, wide pit (c) Elliptical pit (d) Vertical grain attack (e) Sideway / Subsurface pit (f) Undercut pit / sub surface (g) Horizontal grain attack [17] 15
Figure 13. Gas composition without H2S production 18
Figure 14. Gas composition with H_2S production 19
Figure 15. Eddy Current Testing 20
Figure 16. Ultrasonic flaw detection device 21
Figure 17. Magnetic particle inspection device 22
Figure 18. Eddy current testing 23
Figure 12. Concentration of H2S in air PPM & its short term & immediate danger to human life 41
Figure 19. Flushing for removal of dirt through water jetting 44
Figure 20. Inspection of tube through RFT and numbering of tubes 45
Figure 21. Dye penetrant testing of partition plate 47
Figure 22. MPI inspection 48
Figure 23. Application of Ultrasonic flow detection 50
Figure 24. Application of Thickness gauging by applying gel as Couplant 52
Figure 25. Application of hardness testing through portable hardness tester 53

Figure 26. (a) Grinding & Polishing of spot area, (b) Diamond paste & Etchant (c) In-situ Metallography of Regeneration Gas cooling & Heating system. 54
Figure 27. (a) Overall view & Saddle support condition of heat exchanger and (b) Name plate with specifications of regeneration system (c) Dye Penetration testing of equipment (d) Insulation pocket for inspection (e) Tube bundle inspection (f) Numbering of tube bundle 56
Figure 28. (a) Internal visual inspection, (b) External Visual Inspection, (c) Inspection condition of Insulation material, (d) Pre-& Post cleaning condition of tube bundles, and (e) Inspection measuring locations. 58
Figure 29. Pictorial display of defects of tube bundle. 60
Figure 30. Dye penetration testing of partition plate 61
Figure 31. Thickness gauging results & comparison 65
Figure 32. Sketch for regeneration gas fooling and heating system 76
Figure 33. 3D overview of regeneration gas heating and cooling system 77

List of Tables

Table 1 Remote field testing of tubes and table 9 & 10 shows the percentage metal loss of tubes observed during inspection. 59
Table 2. Type of defects in tube bundle 59
Table 3. Dye Penetrant Inspection 61
Table 4. Magnetic particle inspection results 62
Table 5. UDF inspection results 63
Table 6. Thickness gauging of dish end, Shell, and Nozzle 64
Table 7. Hardness Testing of Base Metal, HAZ and weld 66
Table 8. In-situ Metallography results 68
Table 9. Produced water Analysis Report 69
Table 10. Calculation for corrosion rate, remaining life, maximum allowable working, and operating pressure 71

Chapter 1:

Introduction

A regeneration gas cooling and heating system is installed in a processing filed of an E & P (Exploration and processing) company for the removal of impurities from natural gas. This system was designed based on initial testing results of the gas composition, however the entry of H_2S poses a sever threat to the integrity of the system. The failure of the system due to H_2S corrosion at elevated temperature, and turbulence potentially leads to loss of production, operational disruptions, safety hazards for the work and nearby areas.

The integrity of the system is to be analyzed with the help of Non-destructive inspection techniques and the results will reveal the corrosion rate, remaining life and maximum allowable working pressure and the next inspection interval. [1]

Hydrogen sulfide (H_2S) corrosion, also known as sour corrosion, is a significant concern in industries such as oil and gas production, refining, wastewater treatment, and certain industrial processes.[2]

This dissertation presents a set of complete investigation into H_2S corrosion in the Re-generation cooling & Heating system, installed in an Oil & Gas field, in two distinct parts. The first part focuses on detailed investigations using both conventional and advanced non-destructive testing (NDT) techniques against H_2S corrosion, aiming to study its effects on the structural integrity of the critical equipment. In the second part, inspection reports are reviewed and analyzed considering the industry codes and standards. The research also involves the calculation of remaining life under H_2S attack, proposes preventive measures, and presents workable solutions to mitigate the effects of H_2S corrosion on the system. By addressing these aspects, this thesis aims to contribute valuable insights into safeguarding equipment integrity, enhancing operational efficiency, and reducing the fiscal impact of corrosion-related expenses across various sectors.[3]

1.1 Background, Scope, and Motivation:

A specific type of process heater is used to convert natural gas into clean and usable gas products. Natural gas typically contains water, which can lead to equipment and component damage. To address this issue, it is essential for the gas to undergo a dehydration process.

The convective heat transfer design of the regeneration gas heater is well-suited for gradually heating the regeneration gas and sending it to the wet desiccant tower to remove moisture from the desiccant. The regeneration gas heaters operate within the temperature range of 450º F to 650º F and can manage pressures up to 1100 Psi. However, there is a risk of tube failures in localized areas of the heat transfer coil due to elevated temperatures at high operating pressures.[4]

Dehydration is necessary for natural gas extracted from production wells or underground storage to protect the distribution system from corrosion and the formation of hydrates. In the commonly used absorption dehydration process, wet gas flows through a pressure vessel tower filled with solid desiccants. The desiccant's surface absorbs moisture, allowing the gas to exit the tower in a dry state. When the desiccant becomes saturated with moisture, another tower with dry desiccant is automatically activated. A re-generation gas heating and cooling system is a heater using synthetic or organic oil which is circulated as a thermal fluid. That thermal fluid heats the regeneration gas through a heat exchanger, which is typically shell and tube or plate and shell. This system is installed at the Gas & LPG (liquified petroleum gas) plant of a reputed Exploration & Processing company and through continuous monitoring of gas composition, H_2S from different wells is expected to enter the system and could cause cracking/rupture and resulting in production loss, losses of human life resulting complete shutdown of plant, Due to un-expected production of H_2S (Hydrogen sulfide) from reservoir, as H_2S being heavier than oil and also the reservoir formation is of limestone and gypsum. ($CaSO_4.H_2O$) Up to 50PPMs (Parts per millions) of H_2S, a protective layer of iron sulfide is formed. The FeS layer of steel is not stable above 50PPMs, it is removed from the steel surface in an acidic environment, forming again H_2S, enhancing corrosion and diffused the steel structure resulting in cracking of steel structure.

Re-Generation gas cooling and heating system is susceptible to H_2S corrosion damage mechanism as the partial pressure is above 0.05 psi at 500 ºF. as per API 580 / 581 Risk- Based Inspection (RBI) code. [5]

When the partial pressure of H_2S (hydrogen sulfide) exceeds approximately 0.05 psi (0.0003 MPa), it can lead to sulfide stress corrosion (SSC) in steels that have a tensile strength of around 90 psi (620 MPa) or higher. SSC can also occur in steels with localized zones of weld or weld heat-affected zone (HAZ) hardness surpassing 237 HB (Brinell hardness), as well as in Cr-Mo (chromium-molybdenum) steel welds that have not undergone post-weld heat treatment (PWHT) or have been inadequately treated.[6]

The value of 0.05 psi for H_2S partial pressure as a threshold for SSC is primarily based on experience in the oilfield industry and is not an exact value. The actual H_2S partial pressure required to cause SSC can vary depending on factors such as steel strength and hardness, pH levels, and stress levels.

To combat the challenges posed by H_2S corrosion, preventive measures must be implemented. This research aims to analyze the impact of H_2S corrosion on the integrity of the regeneration gas cooling and heating system using both intrusive and non-intrusive inspection techniques.[7]

Corrosion-related costs can vary significantly across industries, locations, and specific assets. These costs encompass direct expenses for maintenance, repair, and replacement of corroded equipment, as well as indirect costs, such as downtime, lost productivity, and environmental damage. While exact global figures are challenging to obtain, corrosion costs are estimated to be substantial, impacting various sectors in the economy.

The case under consideration involves a comingled flow of gas originating from 11 different wells in the oil and gas industry. The extremely critical equipment, namely the Re-generation gas cooling and heating system, is threatened by H_2S corrosion. The primary purpose of this equipment is to remove impurity gases like CO_2 and H_2S. Although the equipment was designed with materials compliant with The National Association of Corrosion Engineers (NACE) standards, the unexpected entry of H_2S has created a different scenario. The original equipment design was primarily focused on countering CO_2 corrosion, making it crucial to ensure the integrity and health of the system through inspection techniques specifically targeting H_2S corrosion. The research follows guidelines from prominent industry standards, including API-510, NACE RP 0175, AMSE section V, Section VIII, API RP-584, API-571, and welding codes & standards API-1169.[3, 4, 8, 9]

The National Association of Corrosion Engineers (NACE) estimates that the oil and gas industry incur billions of dollars in corrosion-related costs annually. These expenses cover measures for corrosion control, maintenance, repairs, and equipment and infrastructure replacement affected by corrosion. Moreover, corrosion significantly impacts various manufacturing processes and industrial equipment, contributing to a country's GDP expenses.[10]

If carbon steel piping and equipment in regenerators and heat exchangers have not undergone post-weld heat treatment and are in contact with amine fluids, they are prone to cracking. Equipment that manages lean amine service is more susceptible to cracking compared to equipment in rich amine service, but it is not necessarily immune. This is especially true for vessels where acid gas enters the amine (resulting in rich amine) or leaves the amine (resulting in lean amine). These conditions increase the risk of cracking in the mentioned carbon steel piping and equipment.[6]

Its observed and noted that heat affected zones (HAZ) and or the weld metal are the sites where Cracks can most often appear but are most often found in the high residual stress zone, which is typically beyond the metallurgical HAZ, about a tenth of an inch or more (several millimeters) from the weld.[6]

1.2 Types of Heat Exchangers Failures:

Transferring heat from one medium to another (liquid, vapor, or gas) is especially important and that is mostly conducted with the help of a heat exchanger system. Where cooling and heating are required, heat exchangers are used for both situations. [11]

There are twelve diverse types of heat exchanger being used as per their specification, however, Shell and tube heat exchanger are in common use in oil and gas processing plants.

1.3 Failure mechanisms:

Corrosion is an electrochemical deterioration of metal and is one of the causes of failure for different equipment in the industry. Commonly observed modes of failure in heat exchangers (HE) include fatigue, corrosion exhaustion, stress corrosion cracking (SCC), and tensile fracturing.[5] Corrosion is a result of mechanical damage to the heat exchanger surfaces caused by the intense interaction with moving fluids and the surrounding atmosphere. The diagram in figure 1. shows the general corrosion mechanisms that occur in metals. Additionally, other mechanical processes play a crucial role in the design, operation, and corrosion of heat exchangers. For instance, corrosion can arise in contacting surfaces between metals that experience vibrations or sliding during loading conditions Fouling and corrosion are outcomes of the operational activity of a heat exchanger (HE) and should be taken into consideration both during the design of a new heat exchanger and while operating an existing one.

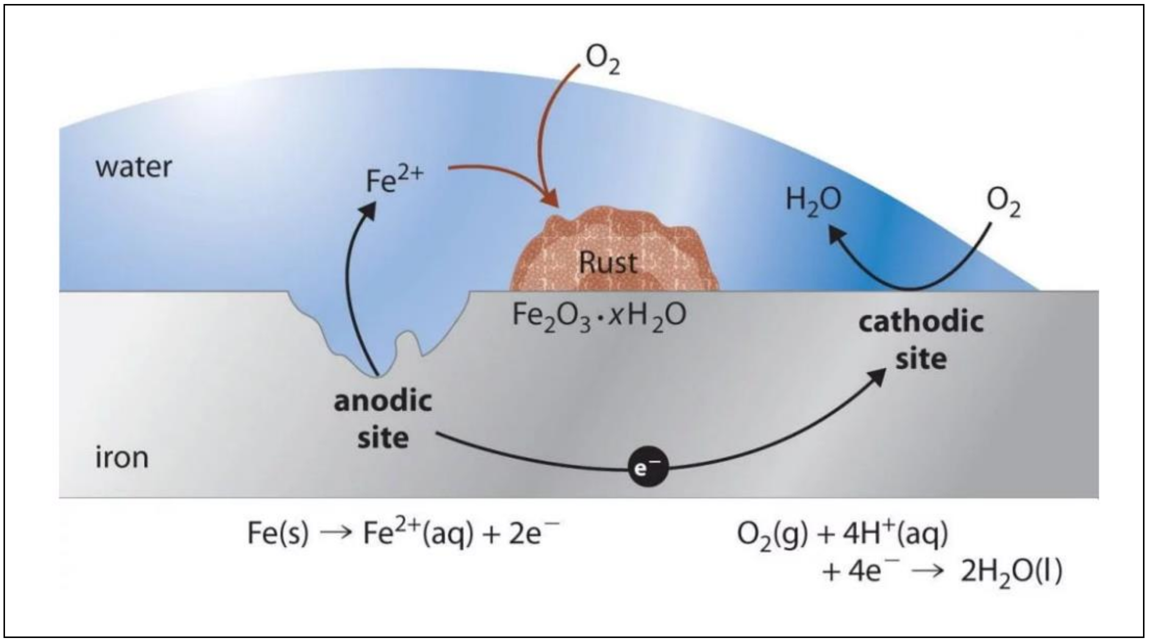

Figure 1. General Corrosion mechanism

1.3.1 Mechanical Failure:

These failures can occur in seven diverse ways: metal corrosion, issues with handling air or water, friction, excessive heat damage, freezing, uneven heat distribution, and insufficient cooling energy.

Corrosion is when a material, often a metal, gradually gets destroyed because of a chemical reaction with its surroundings. It happens when the material is exposed to moisture, oxygen, acids, or other chemicals. When a material gets scratched, dented, or abraded, its protective layers can get compromised, making it easier for corrosion to occur. For instance, if a metal surface has a scratch, the metal underneath becomes exposed to the surrounding environment, allowing moisture and oxygen to react with it and cause corrosion. Similarly, a dent in a metal surface can create weak points where corrosion can happen more quickly.[12] Hence, it is crucial to consider both mechanical damage and corrosion when designing and maintaining materials and structures, particularly in environments where corrosion is prone to happen. By considering these factors, appropriate measures can be implemented to prevent or mitigate the detrimental effects of mechanical damage and corrosion, ensuring the durability and longevity of the materials and structures.

1.3.2 Metal Erosion:

Harmful corrosion can occur when metals are released from the piping due to excessive fluid flow rates in either the heat exchanger shells or the tube side. As corrosion damages the protective layers of the tubes, fresh surfaces are exposed and further susceptible to invasion. This can be accompanied by erosion, particularly in areas where erosion is already present.[12]

The recommended optimal velocity in pipes and inlet nozzles depends on numerous factors such as tube size, treated fluid, and heat conditions. Materials like titanium, stainless steel, and aluminum-nickel can withstand higher fluid velocities compared to copper. Figure 2 illustrates the occurrence of erosion, erosion corrosion, and accelerated corrosion in flange, elbow, and U-curve regions of equipment. Among these areas, the U-curve of U-type heat exchangers and duct openings are particularly prone to erosion. Copper is limited to a maximum velocity of 7.5 feet per second (fps), while other components can manage velocities of 10 to 11 fps.[13]

When water flows through copper pipes, the velocity will typically be lower than 7.5 fps, regardless of whether the water is pure or contains suspended particles.

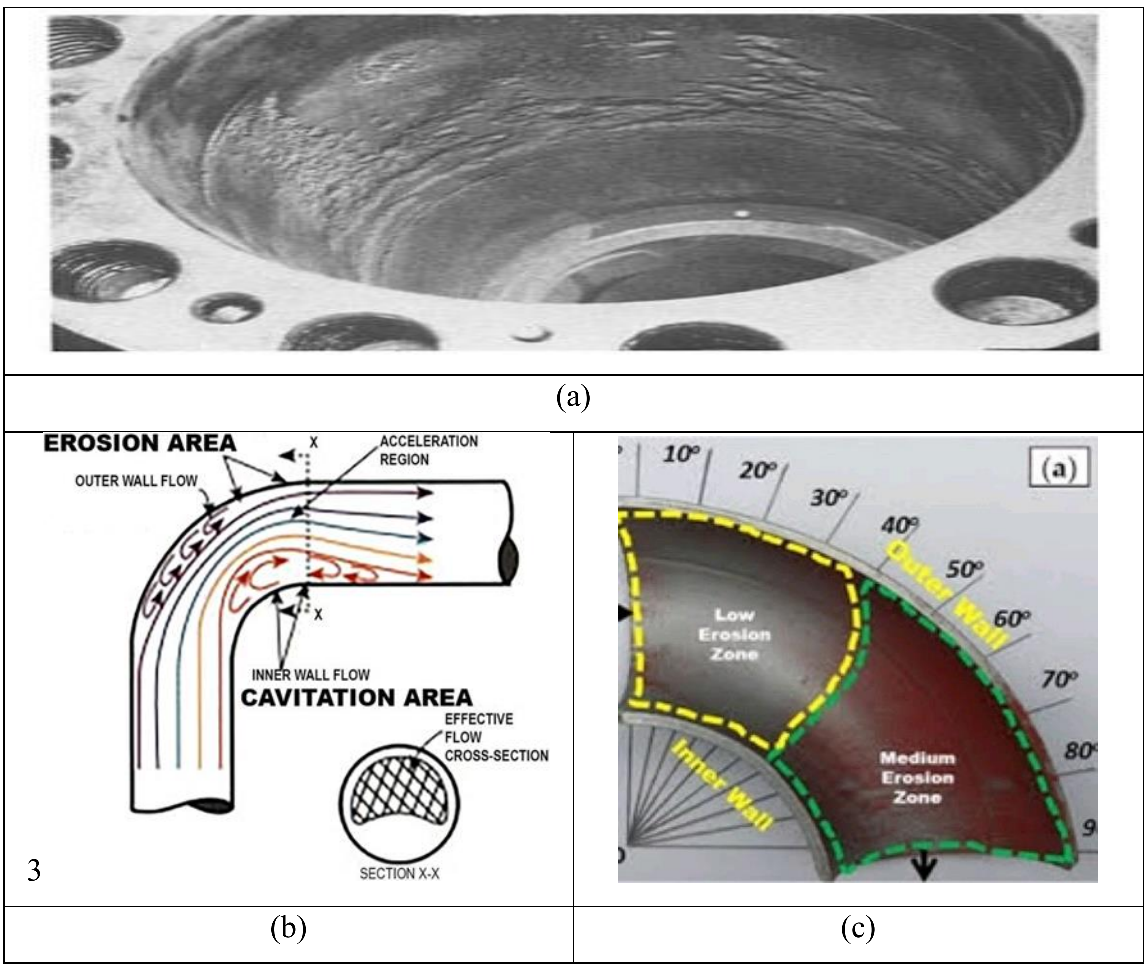

Figure 2. (a) Metal Erosion & (b) Erosion corrosion (c) Accelerated corrosion

1.3.3 Flow Velocity Effect:

In a sour crude gathering line, when the fluid velocity is low, FeSx (iron sulfide) has a greater chance to settle. The galvanic effect between FeSx and the pipe material can significantly accelerate the corrosion process. This means that the corrosion rate will increase rapidly, leading to potential damage and deterioration of the pipeline. It is important to consider the impact of low fluid velocity and the presence of FeSx in the design and maintenance of such pipelines to mitigate the risk of accelerated corrosion.[13]

1.3.4 Vibration:

Tube collapse, which can manifest as strain stress cracks or degradation, can occur at the contact points with baffle plates. This issue is primarily caused by excessive friction generated by equipment like air compressors or cooling machines. Such movements should be prevented in heat exchangers. It is important to note that shell-side liquid velocities exceeding 4 feet per second (fps) can induce detrimental tubular vibrations, resulting in a slicing motion against baffle plates. Figure 3 shows the noise and vibration due to high velocity fluid movement in a pipeline and figure 4 shows the failure mode in a pipeline due to the noise and vibration. Fatigue failures are frequently initiated by vibrations caused by excessive flow rates, leading to the hardening of the piping at multiple baffle contact points or in U-bend areas, culminating in a fatigue fracture. [4]

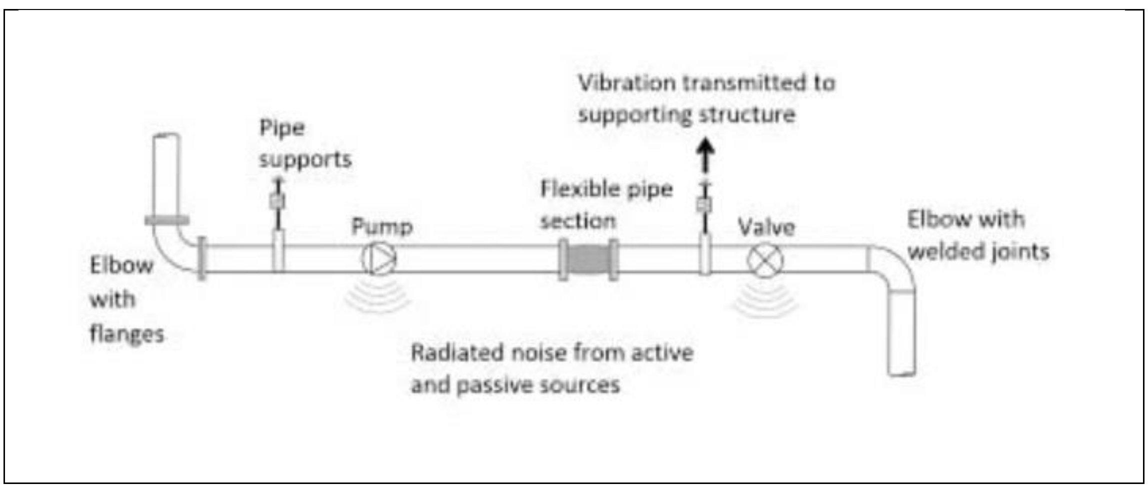

Figure 3. Noise & vibration in fluid pipe

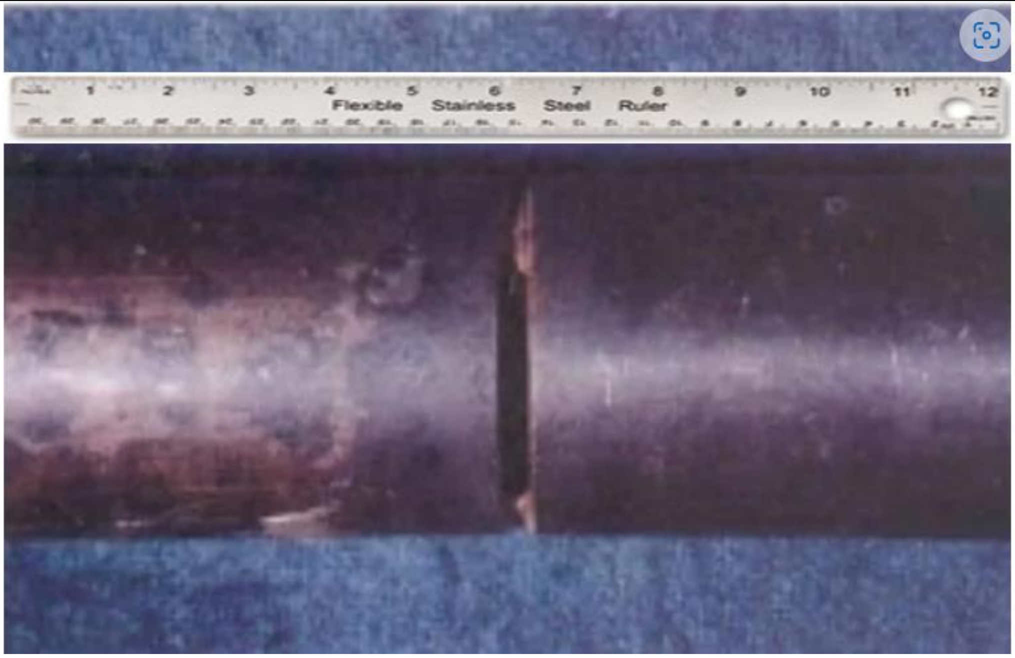

Figure 4. Vibration induced split.

1.4 Galvanic Effect:

FeSx is highly conductive, which can lead to galvanic corrosion of steel as it acts as a cathode. Figure 11 illustrates the initiation of galvanic corrosion in various metals. When the FeSx layer starts to spall, exposing a small anodic surface (steel) in a larger cathodic area, it can result in severe pitting corrosion.

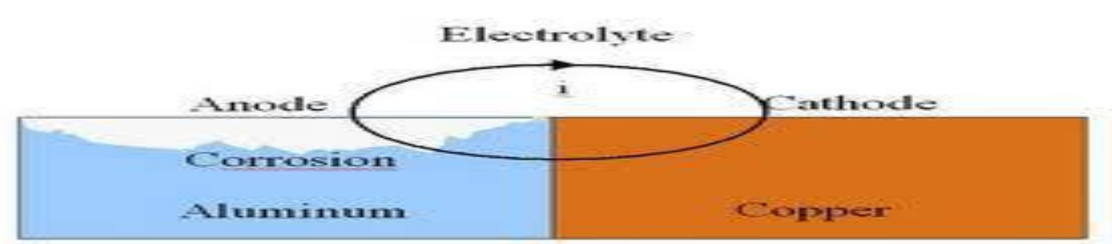

Figure 5. Galvanic Corrosion

1.5 Thermal fatigue:

The cumulative stresses caused by repetitive heat treatments, particularly in the U-bend region, can lead to tubing failure due to induced fatigue. This issue is further complicated by the temperature variation along the U-bend conduit, with a decrease in temperature. Figure 5. Below shows the thermal fatigue failure damage mechanism and crack propagation in a metal. As the temperature changes, the tube undergoes bending, creating a force that operates within the material's compressive limits before cracks develop.[12]

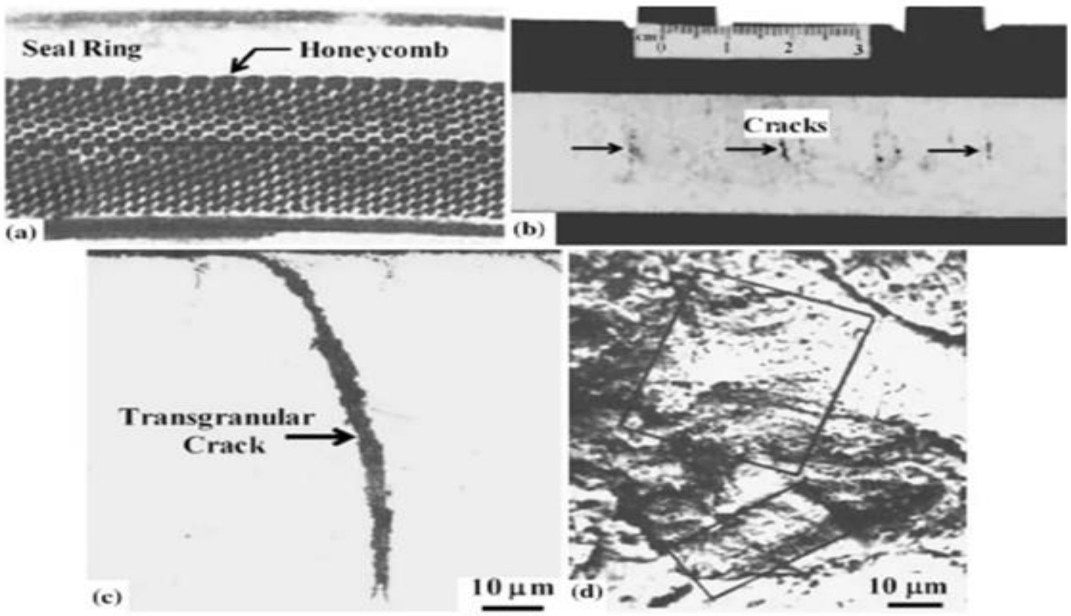

Figure 6. Thermal Fatigue

1.6 Chemical Induced Corrosion:

Iron and its alloys are susceptible to corrosion when exposed to external factors such as soil, climate conditions, liquids, or aqueous solutions. Corrosion refers to the degradation of these materials. In various industries, corrosion is a significant contributor to premature equipment failure, leading to issues like costly breakdowns, unexpected shutdowns, and repair expenses. Figure 6 illustrates the chemical-induced corrosion occurring in metal tubing. The drop in wet vapor pressure is a significant factor contributing to uniform corrosion and erosion-corrosion, resulting in the deterioration of unalloyed metals. Even without water droplets, the flowing medium can still have a corrosive effect on the initial baffle. Uncoated steel has limited resistance to corrosion, making it susceptible to corrosion from exposure to water vapor and chemicals. To mitigate this, protective coatings are used to prevent corrosion in such situations. [12]

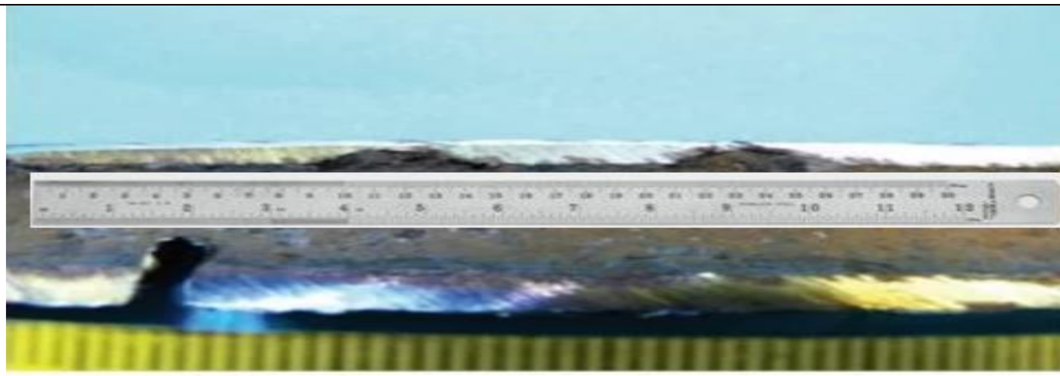

(a)

(b)

Figure 7. (a) X-section of tubing damage via pitting (b) Uniform corrosion

Pharmaceutical factories, the oil industry, offshore and onshore electrical power plants, the paper industry, air conditioning and refrigeration systems, as well as food and beverage production facilities, are all experiencing a gradual increase in corrosion-related challenges. Figure 7 shows the intergranular and crevice corrosion in gasket of heat exchanger. Acquiring a basic understanding of the corrosion process can be beneficial for improving operations and implementing effective solutions. The overall rate of corrosion is influenced by several factors, including the condition of the substances involved. To reduce the risk of corrosion, several criteria can be followed. These include maintaining appropriate temperature conditions, controlling the pH level to keep it low, managing residual chlorine levels, monitoring, and controlling high levels of total dissolved solids (TDS), using materials with high durability, minimizing water vapor density, monitoring variations in the flow system, and controlling the concentration of strong ions like sulfate, nitrate, chlorine, oxygen, and titanium. Considering these factors can help mitigate issues related to corrosion in various industries. [7]

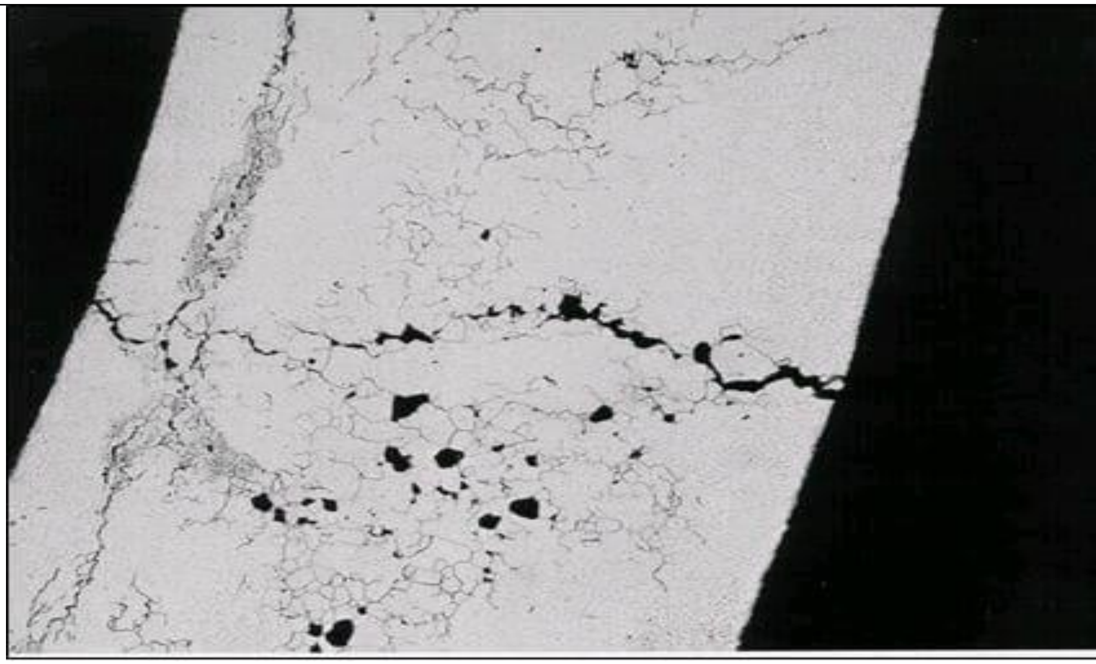

(a)

(b)

Figure 8. (a) Intergranular corrosion (b) Crevice corrosion under gasket of plate heat exchanger

1.7 Fouling and corrosion:

Fouling refers to the unwanted accumulation and buildup of materials on the surfaces of machinery and tools. This accumulation typically consists of low thermal conductivity materials, which form a layer that hinders the efficient transfer of thermal energy in a heat exchanger. Figure 8 illustrates the initiation of the fouling process through the movement of ions, deposition, and subsequent removal. The presence of fouling results in increased resistance to fluid flow, leading to higher pressure drops across the heat exchanger. Fouling can have significant financial implications for industries, including increased fuel consumption, reduced operational efficiency, decreased output, and higher operational expenses. [14]

The fouling process can be broken down into five main steps: fouling activation, surface transfer, surface attachment, surface growth, and surface maturation. Several variables play a role in influencing the fouling process, including pH, density, temperature, surface composition, and friction. Having a clear understanding of these factors and their effects on fouling is essential for developing effective strategies to minimize issues related to fouling. By addressing these variables, industries can mitigate the impacts of fouling and optimize the performance and efficiency of their equipment and processes.[12]

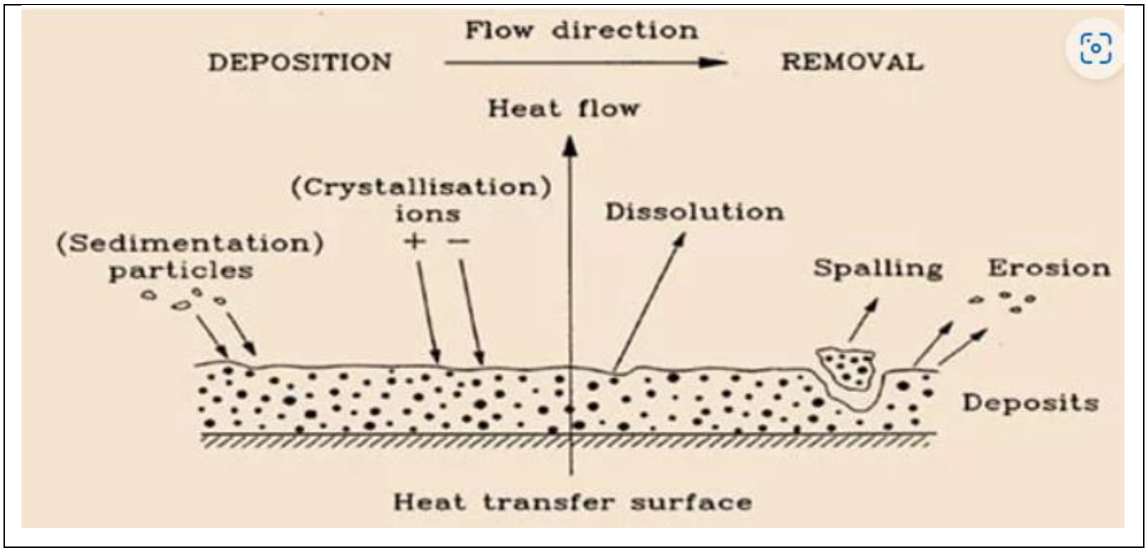

Figure 9. Fouling process

In recent years, there have been advancements in techniques aimed at reducing fouling and preventing corrosion. Previously, chromate was commonly used as a chemical product for corrosion prevention and crystal manufacturing preservation. However, due to environmental concerns, the use of chromate-based additives has been banned or restricted. To replace chromate-based additives, corrosion inhibitors such as polyphosphates have been introduced. Polyphosphates function as effective corrosion inhibitors by forming a protective layer on metal surfaces, reducing the risk of corrosion, and prolonging the lifespan of equipment. [15]

These advancements in corrosion prevention techniques and the development of alternative additives help industries mitigate the risks associated with fouling and corrosion, leading to improved operational efficiency and cost savings.

1.8 Mesa Corrosion:

Mesa corrosion is one of the types of corrosion that occurs when low alloy steels and carbon steel are exposed to wet carbon dioxide conditions at elevated temperatures. This leads to the growth of an iron carbonate surface layer, which acts as a shielding barrier against further corrosion.[16]

Mesa corrosion is characterized by the presence of sharp pits or holes that resemble the Mesa Mountains in the United States. These pits are formed when the protective corrosion films on the steel surface experience localized breakdown. The sharp edges holes in messa corrosion are reflected in figure 9. The occurrence of mesa corrosion is particularly evident during the CO_2 corrosion of carbon steel.

Several factors can contribute to the local breakdown of the protective films, including temperature ranges of 104°F to 176°F, CO_2 partial pressure of 1.8 bar, a pH level of 5.8, high iron content in the water, and flow rates ranging from 0.1 to 7 m/s. Studying these influencing factors is crucial for understanding and managing mesa corrosion to prevent its detrimental effects on steel equipment and structures.[16]

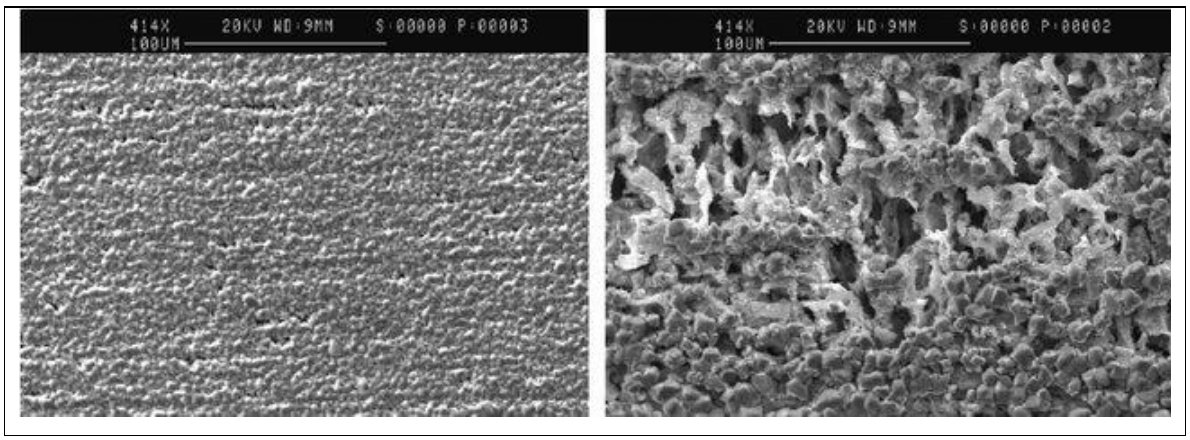

Figure 10. Mesa corrosion sharp edges holes

1.9 Pitting Corrosion:

Pitting corrosion is a particular type of corrosion that causes the formation of small "holes" or openings in the material. It is more destructive than uniform corrosion because it is harder to detect, predict, and protect against. Pits are often hidden by corrosion products, making them visually challenging to identify.

Even a small and narrow pit with minimal overall metal loss has the potential to lead to the failure of an entire engineering system. Pitting corrosion can manifest in different forms, resembling several types of localized corrosion attacks. Pits can be partially covered or have exposed openings, and they can exhibit shapes like hemispheres or cups.[17]

Figure 10 shown below reflects the Narrow, deep pit (b) Shallow, wide pit (c) Elliptical pit (d) Vertical grain attack (e) Sideway / Subsurface pit (f) Undercut pit / sub surface (g) Horizontal grain attack.

The insidious nature of pitting corrosion underscores the importance of comprehensive monitoring, preventive measures, and appropriate materials selection to mitigate its destructive effects on structures and equipment.

Pitting is initiated by:

i. Localized chemical or mechanical damage to the protective oxide layer can result in the dissolution of a passive film. Water chemistry conditions such as acidity, low dissolved oxygen concentrations (which destabilize the protective oxide film), and high chloride concentrations can contribute to this process. For example, in seawater, these conditions can lead to the breakdown of the passive film and subsequent corrosion.

ii. Damage to a protective coating in specific areas or incorrect application

iii. The presence of irregularities, such as nonmetallic inclusions, in the metal structure of the component.

The formation of a pit can be triggered by the presence of an unusual cathodic site within a normal surface, where a previous pit has corroded, or by an abnormal anodic site surrounded by a normal surface that acts as a cathode. In such cases, a localized electrochemical cell is formed, leading to the initiation of a pit.

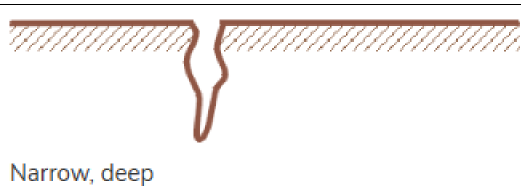	
(a)	(b)

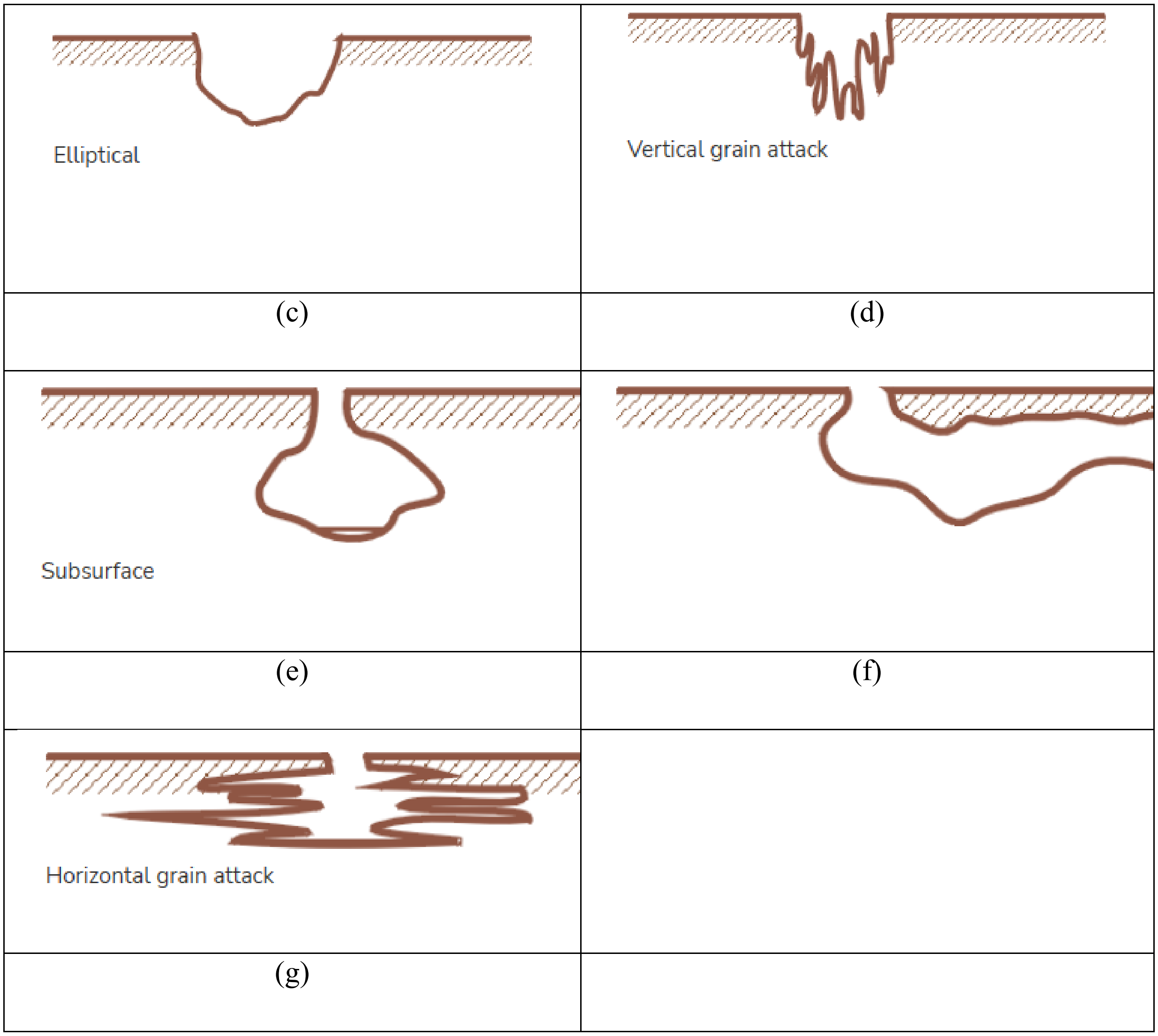

Figure 11. (a) Narrow, deep pit (b) Shallow, wide pit (c) Elliptical pit (d) Vertical grain attack (e) Sideway / Subsurface pit (f) Undercut pit / sub surface (g) Horizontal grain attack [18]

Corrosion pits can cause damage beyond localized loss of material thickness due to their role as stress risers. At the bottom of these pits, fatigue and stress corrosion cracking can initiate and propagate. Even a single pit in a large system has the potential to lead to catastrophic failure. Recent events in Mexico serve as a tragic example of such failures, where 215 people lost their lives due to a single trench in a gasoline line that crossed a sewer line.[17]

1.10 Sources of hydrogen sulfide:

H_2S (hydrogen sulfide) is naturally produced through the decomposition of organic matter by bacteria. This can happen in environments with low oxygen levels, such as swamps and polluted water. H_2S is also present in natural gas, petroleum, sour crude oil (which contains more than 0.05% sulfur), sulfur deposits, volcanic gases, and sulfur springs.

Indeed, H_2S can also be produced during various industrial processes. It is important for individuals working in the industry to be aware of the potential exposure to H_2S while performing their duties. The petroleum industry, including oil and gas wells, refineries, natural gas plants, and pipelines, takes H_2S exposure seriously.[19]

In chemical manuals, H_2S may be referred to as sulfuretted hydrogen, hydrogen sulfide, hydro sulfuric acid, or dihydrogen sulfide. Due to its toxic nature, the Environmental Protection Agency (EPA) has classified H_2S as hazardous waste, and its concentrations are measured in parts per million (ppm) or percentages.

H_2S can react with strong oxidizers, bleach, and hydrogen peroxide, which can lead to fire, explosions, or damage to metals. When H_2S is burned, it produces toxic SO_2 gas. Additionally, H_2S can form metal sulfides that have the potential to spontaneously ignite upon exposure to air. When H_2S is dissolved in water, it forms a weak acid that can corrode metals like steel, carbon steel, copper, silver, brass, and bronze. It is important to manage and store H_2S safely to prevent these hazardous reactions and protect against metal corrosion.

1.11 H_2S Corrosion:

Corrosion caused by H_2S is a specific form of aqueous corrosion that can affect various upstream equipment exposed to H_2S. This includes downhole well tubing, flowlines, transport pipelines, and processing equipment. The presence of H_2S in the environment can lead to corrosion-related issues in this equipment, emphasizing the need for appropriate measures to prevent or mitigate H_2S-induced corrosion.[5]

All internal surfaces that encounter water are susceptible to H_2S corrosion. This can occur due to the presence of produced water in the lower part of the line or condensed water in the upper part of the line. Under-deposit corrosion is a specific form of corrosion that can occur in areas where solid particles settle, and deposits accumulate. These localized attacks are a result of corrosion happening beneath the deposits or within them. It is important to address and manage under-deposit corrosion to prevent further damage to the equipment and ensure its proper functioning.

Corrosion caused by H_2S can be extremely aggressive and lead to rapid and extensive damage. To mitigate the effects of H_2S corrosion, specialized stainless alloys can be used as a substitute for traditional steels. These alloys, when coupled with corrosion inhibitor chemicals, can be particularly effective in combating H_2S corrosion. However, it is important to note that these alloys can be expensive due to their requirement for excellent corrosion resistance properties and resistance to other forms of associated attacks, such as sulfide stress corrosion cracking. The inflated cost is justified by the need to ensure long-term protection and durability in H_2S-rich environments.[5]

H_2S can be present naturally in reservoirs or generated through chemical and biological reactions. One example is the phenomenon known as souring, which occurs when water re-injection into a field leads to the growth of Sulphate Reducing bacteria (SRB) in the oil and gas industry. These bacteria contribute to the production of H_2S, impacting the souring of the field. It is important for the oil and gas industry to be aware of and manage the presence of H_2S in such situations to ensure safety and prevent corrosion-related issues.

In studies investigating localized corrosion, the impact of exposure time and surface area was examined to determine if there was a higher likelihood of observing localized corrosion. In experiments conducted near the saturation point for iron carbonate in solution, localized corrosion was observed after 30 days. Consequently, the experimental exposure period was set at 30 days, and coupons were removed every 10 days for analysis. Furthermore, a coupon with a surface area of 7.2 cm^2 was introduced in the experimental process to address concerns that the previously used 1.0 cm^2 coupon surface may have played a significant role in the development of localized corrosion. Electrochemical Impedance Spectroscopy (EIS), potentiodynamic polarization, multi-component Pourbaix diagrams, and microstructure characterization techniques were employed to study the corrosion of 304L and 316L stainless steel in an oxygen-free solution containing Na_2SO_4 and Na_2S at a pH of 3 and a temperature of 140º F.

The results showed that 316L stainless steel exhibited a lower corrosion rate compared to 304L stainless steel under similar conditions. This was attributed to the denser nature (1.5 times denser) and smoother surface (6% smoother) of 316L. These findings were supported by scanning electron microscope (SEM) images.

The presence of H_2S increased the critical current density for 304L stainless steel and the passivation current density for 316L stainless steel during polarization testing. X-ray Diffraction (XRD) analysis revealed that the higher passivation current density observed in 316L stainless steel was associated with the simultaneous preservation of FeS_2-MoS_2 compounds.

The study suggested that H_2S exposure might hinder the proper functioning of 304L stainless steel in the passivity region. These findings provide insights into the effects of H_2S on the corrosion behavior of stainless steels.[20]

In general, H_2S corrosion tends to result in less aggressive metal thinning for mild carbon steel. This is because the corrosion products of H_2S, specifically FeSx (including Mackinawite and Pyrrhotite), have a compact structure that inhibits further reaction of the metal with the corrosive agent (H_2S). These corrosion products function as a protective layer, limiting the extent of metal degradation caused by H_2S corrosion.

1.12 Analysis of H_2S in the regenerator gas cooling and heating system:

A re-generation gas heating and cooling system has been installed at the Gas and LPG (liquefied petroleum gas) facility of a reputable E& P (Exploration and processing) firm. The graph shown in Figure 13 reflects the gas composition without H_2S in oil and gas commingled flow and figure 14 show the parts per million of H_2S in upstream of regeneration gas cooling and heating system. [21] Due to the unexpected formation of H_2S from the reservoir (H_2S being heavier than oil), the presence of H_2S was deducted and was through tube method. Production of H_2S is detailed with comparison in the graph below.

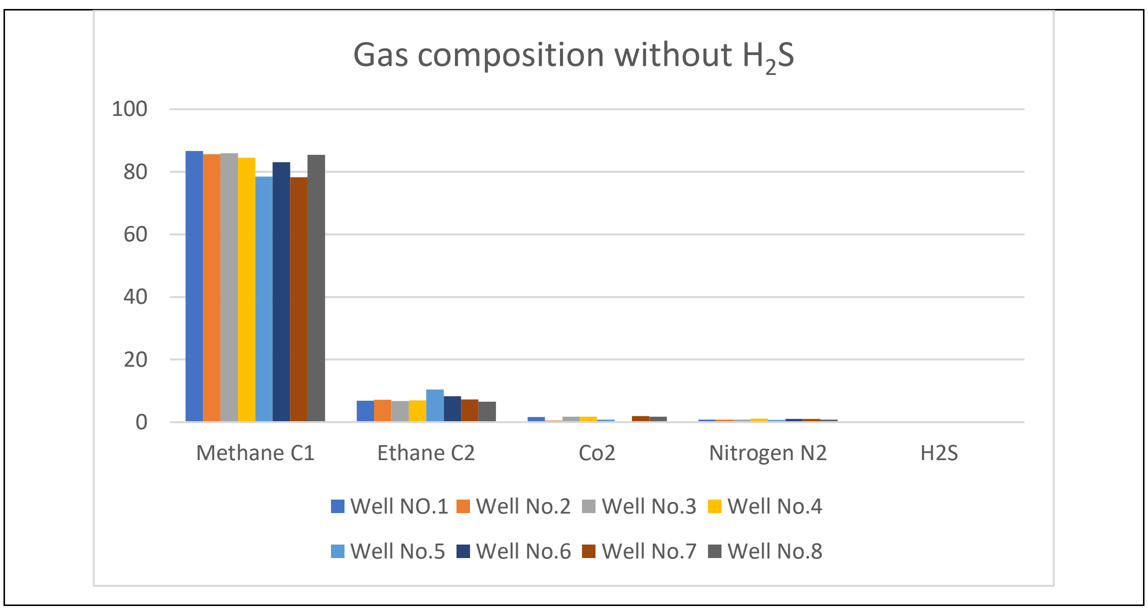

Figure 12. Gas composition without H2S production

During periodic lab test, it was observed that H_2S is being produced from reservoir and lab test revealed the presence of H_2S.

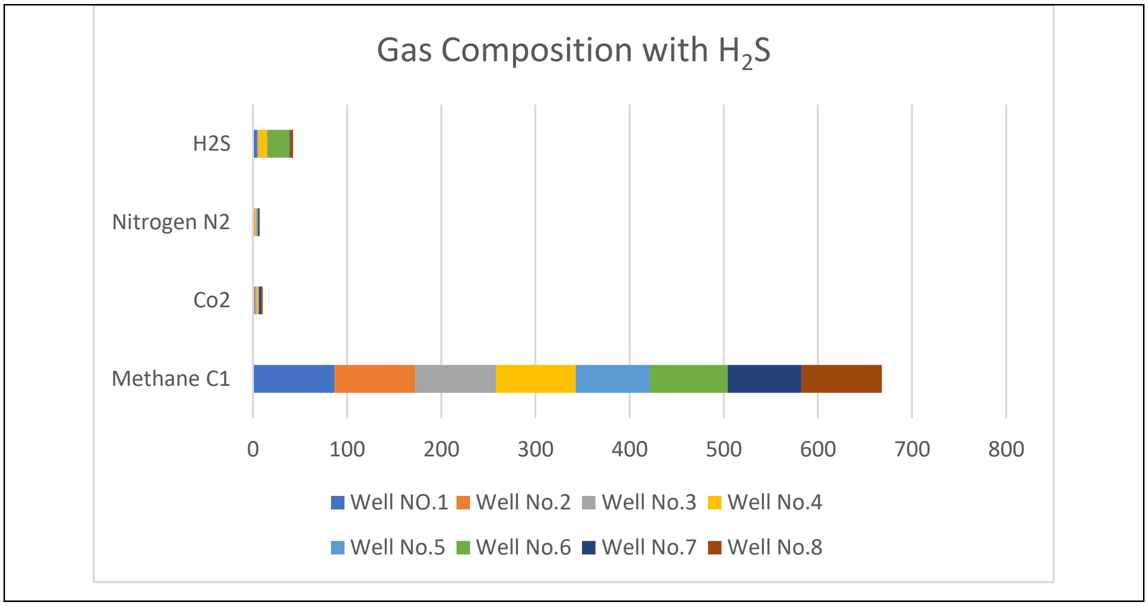

Figure 13. Gas composition with H_2S production

1.13 Conventional & advanced NDT techniques:

Inspection techniques which can be applied for the integrity assessment of any asset, vessel, plant equipment and piping are available. Selection of these inspection techniques depends on the application, damage mechanism, material and the type of defects wanted to be analyzed. These inspection techniques have their own limitations. Some of the inspection techniques can only identify the surface defects, some can identify sub – surface defects and some can identify the near surface defects.[22]

Some of these inspection techniques have been explained in this section.

1.13.1 Using Remote Field Eddy Current Testing to Detect Stress Corrosion Cracks in Gas Transmission Pipelines:

To inspect conductive material for defects, such as cracks, corrosion, or changes in material properties, remote field eddy current testing a non-destructive technique is widely used. Specifically ferromagnetic materials like iron & steel are inspected through this technique. Remote field eddy current testing (RFEC) is a non-destructive technique that can be used to detect deeper flaws which cannot be inspected through conventional ECT. It is a typical NDT technique for inspecting metal pipelines. Sacillo et al, presented a measurement system that can be used to find flaws in an ASTM A-36 steel pipe with the help of tangential and regular MMM signals.[23]

Numerous tubes were found to have corrosion, erosion, wear, pitting, and cracking because of prolonged in-service operation when inspected through this technique. Repairing these tubes through will not only help to reduce the downtime but also will ensure the health of the system and safe operation of the plant. Inspection of these tubes through conventional method is quite difficult. To effectively monitor small-bore tubing, the local petrochemical industry has now executed and is deploying field-portable inspection devices.

With the help of four NDT techniques which include remote field eddy current testing (RRFT), eddy current testing (ET), magnetic flux leakage (MFL) and ultrasonic internal rotating inspection device. One computer with supporting hardware and software powers them all. The approach is extremely fast and around 400 tubes per day can be inspected.

For nonconductive materials, as well as ferrous and nonferrous structures can be inspection by IRIS. With the help of IRIS, tube diameter ranging (ID 14.5-76 mm), and wall thicknesses (1.25-8.0 mm) can be inspected to identify corrosion and to thin based on the OD tube, this technique can also help to detect the defects which are under some support or under some insulation.[23]

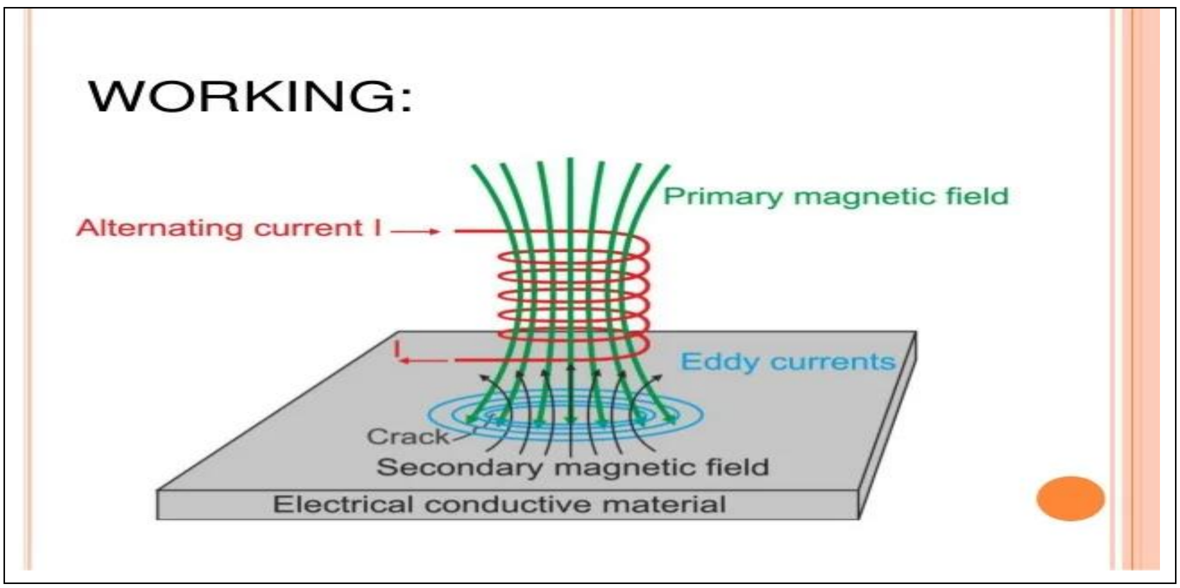

Figure 14. Eddy Current Testing

1.13.2 Ultrasonic flaw detection:

High- frequency sound waves are used in ultrasonic flaw detection technique to detect flaws or defects in a materials detection which is a non-destructive testing technique. In this technique, high -frequency sound waves propagate through the material which is to be inspected and this high frequency wave is generated through a transducer. When these waves encounter a flaw or defect, some of the energy is reflected to the transducer, which can then be detected and analyzed to determine the presence, location, and size of the flaw.

Ultrasonic flaw detection is widely used in the inspection of metals, plastics, ceramics, and other materials for various applications, including quality control, maintenance, and safety. Some common applications of ultrasonic flaw detection include inspecting welds, detecting cracks, measuring wall thickness, and identifying material defects.[24]

The advantages of ultrasonic flaw detection include its non-destructive nature, high accuracy, and ability to detect both surface and subsurface defects. It can also be used to inspect materials of various shapes, sizes, and thicknesses. However, it requires skilled operators and proper equipment calibration to achieve accurate and reliable results. The ultrasonic flaw detection meter used during the inspection is shown in figure 16.

All the welding joints and Heat affected Zones (HAZ) and Tee joints of the equipment is to be made clean through the wire brush paint / coat was removed to make the surface exposed with the flaw detector. The probe of the ultrasonic flaw detector is to be placed as per procedure provided by the OEMs to investigate the flaws in the surface, weld joints and T joints. Data is collected and stored in the inbuilt storage capacity of the ultrasonic flaw detector for further analysis.

Figure 15. Ultrasonic flaw detection device

1.13.3 Ultrasonic thickness gauging:

High frequency sound waves are generated to measure the thickness of any material through this nondestructive inspection technique. The equipment used for ultrasonic thickness gauging is shown in figure 16. To perform ultrasonic thickness gauging, ultrasonic thickness gauge is required, which is a handheld device that generates and receives ultrasonic waves. [24]

1.13.4 Magnetic particle inspection:

A nondestructive inspection technique which is used to detect the surface and near-surface flaws of any ferromagnetic materials. This technique is widely used in the oil and gas industry, refineries, automotive, manufacturing, and aerospace.[24]

The process of magnetic particle inspection involves the following steps:

i. Magnetization: The object or component to be inspected is magnetized. This can be achieved by either applying a magnetic field through direct magnetization (using a magnetic yoke or permanent magnets) or by using an electromagnetic coil to induce a magnetic field.
ii. Application of Magnetic Particles: Small iron or iron oxide particles are applied to the surface of the magnetized object. These particles can be in dry form or suspended in a liquid carrier such as oil or water.
iii. Flaw Detection: flaw detection is conducted when these magnetic particles are drawn to the areas of magnetic flux leakage caused by surface or near-surface defects, such as cracks, voids, or discontinuities. The shape and location of the flaw is highlighted as these particles accumulate and make a visible indication.

Figure 16. Magnetic particle inspection device

1.13.5 Eddy current testing and Remote field testing:

Internal examination of ferromagnetic tubes, such as those in a carbon steel steam exchanger, is typically done using remote field testing (RFT). It uses Eddy Current technology and is an electromagnetic NDT technique. It makes use of transmitter coils to produce a magnetic field that passes through and out of the tube wall before returning to the tube to strike the reception coil. Magnetic particle inspection tool / equipment is shown in figure 18.While tube thinning can be detected using the absolute mode, the differential mode of Remote Field Testing provides for more accurate fault detection (corrosion, erosion).[23]

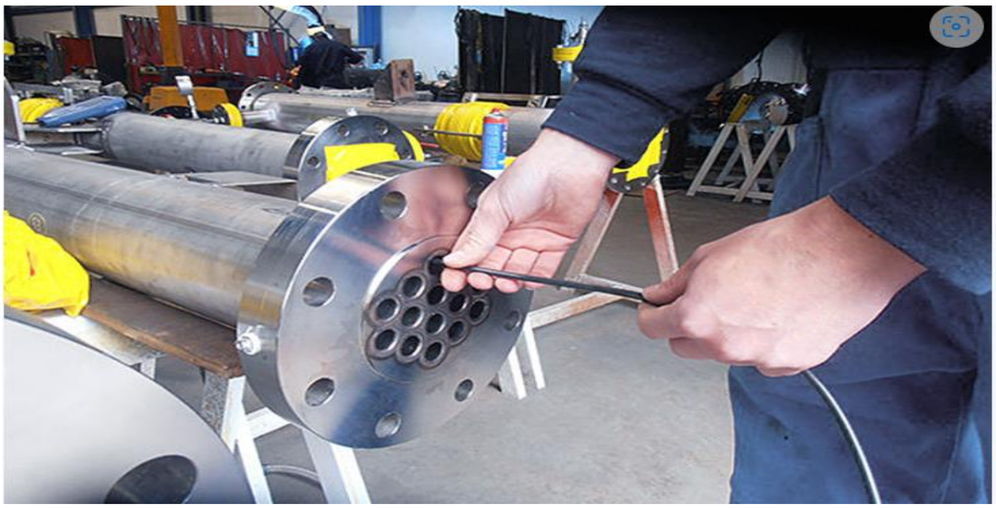

Figure 17. Eddy current testing

The calibration of the probe is carried out prior to inspection of tube bundles to ensure the accuracy of the testing, Internal and external cleaning of tube bundle is carried out through the water flashing and after the confirmation of cleaning procedure, marking of each tube in the tube bundle is marked to ensure and confirm the back tracing of inspection report. Figure 19 shows the eddy current testing equipment. Eddy current was inserted in each of the tubes and the results were collected through the data cable and attached screen and the inspected data was recorded in the machine for further review through the available defect library.[23]

1.13.6 Metallography by Portable microscope techniques:

Metallography is important equipment used in materials science and engineering to analyze and assess the microstructure, properties, and performance of various materials, including metals and alloys. These techniques provide valuable information into the structural characteristics and behavior of the materials under investigation.[9]

Portable inspection techniques provide an advantage of inspecting the microstructure on site as it is not possible to take the exact sample of the material from the equipment and prepare for metallography, therefore metallography provides the best possible solution for the integrity assessment of the equipment through confirming any changes in the microstructure of material and provides sub-surface defects in a simple way with the help of portable metallography microscope.[9]

Metallography involves the preparation of thin sections or polished surfaces of materials, which are then examined under a microscope. This process allows for detailed observations of the microstructure, including grain size, phase distribution, and the presence of any defects or imperfections. Metallography can provide information about material composition, heat treatment effects, mechanical properties, and the occurrence of corrosion or other forms of degradation.

1.14 Objective of research work

The primary objective of this research is to conduct a comprehensive health and mechanical integrity assessment of the regeneration gas cooling and heating system. The evaluation will be performed under specific operational conditions, namely, exposure to 30 parts per million (PPMs) and 3.75 partial pressure of hydrogen sulfide (H_2S) at elevated temperatures.

The research will involve several key analyses, including the determination of the short-term corrosion rate, estimation of the remaining operational life of the equipment, assessment of the maximum allowable working operating pressure (MAWP), and an in-depth analysis of the potential anticipated corrosion attack caused by H_2S. These assessments will provide crucial insights into the system's performance, safety, and longevity under the specified conditions, aiding in informed decision-making and maintenance strategies.

Chapter 2:

2 Literature Review

Extensive research has been conducted to investigate and determine the root causes of H_2S corrosion in the oil and gas industry, as well as the numerous factors that contribute to its acceleration. Researchers have dedicated significant efforts to understand the mechanisms and behaviors of H_2S corrosion, aiming to develop effective strategies for prevention and mitigation.

Numerous studies have explored the consequences of environmental conditions, such as temperature, pressure, pH levels, and the incidence of other corrosive agents, on the rate and severity of H_2S corrosion. By examining the interactions between H_2S and dissimilar materials commonly used in the industry, researchers have gained valuable insights into the corrosion processes and the specific vulnerabilities of certain alloys and coatings. [25]

Furthermore, investigations have been conducted to identify the impact of operational factors, including fluid flow rates, turbulence, stress levels, and the presence of impurities or contaminants, on the initiation and propagation of H_2S corrosion. These studies aim to provide a comprehensive understanding of the complex dynamics that contribute to corrosion-related failures in oil and gas infrastructure.

In addition to exploring the root causes and factors influencing H_2S corrosion, researchers have also focused on developing advanced monitoring and detection techniques. This includes the use of corrosion sensors, non-destructive evaluation methods, and predictive modeling approaches to assess the condition of equipment and predict potential corrosion-related issues.[26]

The findings from these research efforts are instrumental in guiding industry practices and informing the development of corrosion mitigation plans. By understanding the underlying processes of H_2S corrosion and its interaction with other factors, the oil and gas industry can implement initiative-taking measures to prevent failures, improve safety, reduce downtime, and optimize operational efficiency. [27]

Researchers have extensively investigated the corrosion damage caused by H_2S through both intrusive and non-intrusive inspection techniques, aiming to detect and assess potential corrosion issues before they lead to failure.

Intrusive inspection techniques involve physically accessing the equipment or infrastructure to directly examine and evaluate the corrosion damage. This can include methods such as visual inspection, ultrasonic testing, magnetic particle inspection, and corrosion coupon analysis. These techniques allow researchers to gather detailed information about the extent and characteristics of corrosion, helping to identify critical areas for maintenance and mitigation.[2, 28]

Non-intrusive inspection techniques, on the other hand, enable researchers to assess the corrosion damage without disrupting the operation or integrity of the equipment. These techniques typically involve the use of advanced technologies such as remote sensing, infrared thermography, electromagnetic inspection, and acoustic emission monitoring. These methods provide valuable information about corrosion behavior and potential areas of concern without the need for physical intervention.

By employing a combination of intrusive and non-intrusive inspection techniques, researchers can obtain a comprehensive understanding of the corrosion damage caused by H_2S. This allows for early detection of corrosion-related issues, enabling initiative-taking maintenance and intervention to prevent failures and ensure the integrity of the oil and gas infrastructure.[24]

The application of these inspection techniques contributes to the development of effective corrosion management strategies and helps the industry make informed decisions regarding maintenance, repair, and replacement of equipment. By identifying and addressing corrosion damage in its initial stages, the oil and gas industry can minimize the risk of failures, enhance safety, and optimize operational efficiency.

The application of these inspection techniques contributes to the development of effective corrosion management strategies and helps the industry make informed decisions regarding maintenance, repair, and replacement of equipment. By identifying and addressing corrosion damage in its initial stages, the oil and gas industry can minimize the risk of failures, enhance safety, and optimize operational efficiency.

2.1 Analysis & Investigation of Failures in regeneration gas heating and cooling system:

On the tubes of heat exchanger, which is a commonly used equipment in the oil refining industry for heat transfer processes, a failure analysis was conducted by Jancler et al. [21] diethanolamine regeneration tower in the naphtha hydrotreating unit of an oil refinery was specially focused for the analysis. ASTM A213 grade 316L tubular material having seventy-eight tubes, with dimensions of 19.05 mm in diameter and 1.65 mm in wall thickness. Aqueous flow of H_2S inside and diethanolamine on the outside and water as a coolant was circulating on the inside. Loss of thickness was observed during a scheduled shutdown after six years of continuous operations of the equipment. It was revealed during visual inspection that the corrosion process started from the outer surface to the inner surface of the tubes. 0.16775 mm/year corrosion rate was recorded through Eddy current testing. Thickness loss and presence of perforated tubes leading to containment loss was confirmed through ultrasonic inspection using the internal rotating inspection system (IRIS. The amine corrosion was the primary source of failure which in the presence of H_2S aggravated by diethanolamine (DEA) concentration exceeding 20 wt. % in the analyzed equipment. These tubes were replaced in October 2019, and it was suggested to mitigate the corrosion problem by diluting solution with washing water which could help to active concentration below 5% by mass in the beam tubes of the heat exchanger.[21]

To check the effect of microstructural changes and phase equilibria on behavior of corrosion and hydrogen induced cracking (HIC) sensitivity of an API X65 pipeline steel, a study has been conducted. . Heat treatment at different temperatures, 1562 °F, 1742 °F, 1922 °F and 2102 °F was conducted to achieve the desired hardness and stress relieving in the said equipment. Field emission scanning electron microscope (Fe-SEM) equipped with energy dispersive X-ray spectroscopy (EDS) was used to gauge the microstructure. Open circuit potential (OCP), Potenio-dynamic polarization and electrochemical impedance spectroscopy (EIS) were used to evaluate the corrosion properties under H_2S Environment. Hydrogen charging of the cathode and conducting the tensile test was used to make assessment of Hydrogen induced cracking sensitivity of. Microscopy analyses showed that the microstructure of the steel is ferritic pearlitic together with the islands of martensite/austenite constituents. Increase in heat treatment temperature can help decrease the amount of pearlite and increase ferrite grains size and stabilize the ferrite content. No corrosion active layer found on the surface of pipe steel. Also, with the help of increasing the heat treatment temperature, Corrosion resistance and reduced sensitivity to micro galvanic localized corrosion is increased. Lowering heat treatment temperature, Sensitivity towards HIC (hydrogen induced cracking) of API X 65 Pipeline is increased. [21]

2.2 Investigating the Influence of H_2S/CO_2 Partial Pressure Ratio on the Tensile Properties of X80 Pipeline Steel:

Influence of H_2S/CO_2 partial pressure ration on the tensile properties of pipeline steel X80, in April 2015, Wang et al [29] conducted a study. To check the mechanical properties, I-e tensile & fracture behavior of a flow line X-80 in which hydrocarbon is flowing with corrosive environment at different PPMs of H_2S/CO_2 at different partial pressures, a Slow strain rate tests (SSRT) were conducted [. A damaged tensile property of X80 steel pipeline was reported in the presence of H_2S / CO_2 environment. The tensile and elongation properties to failure of X 80 decreased with increasing partial pressure ratio of H_2S / CO_2. Ductile to brittle rupture was revealed after reviewing the Morphology of rupture. It is noted that Quasi - cleavage features of fractured area increased with increased partial pressure of H_2S / CO_2 at different partial pressure ratios of H_2S / CO_2 diverse types of secondary cracks were identified in SSRT specimen in a corrosive environment. [29]

2.3 Failure Analysis of Type 304 Stainless Steel Amine Exchanger Sheets in a Gas Sweetening Plant:

A failure analysis on the type 304 stainless steel amine exchanger sheets in a gas sweetening plant In August 2017, was conducted by H. Panahia et al. [30] for removing acid gases from natural gas, amine treating has become a popular method due to its advantages, such as high efficacy, prompt acid gas absorption rate, and recyclability. As the heat exchange between the lean & rich amine solution is possible through amine exchanger, it plays a crucial role in this process. However, corrosion is a big challenge in amine gas sweetening plants, due to the presence of corrosive gases CO_2 & H_2S in the natural gas stream. Carbon steels are more susceptible to general corrosion, whereas stainless steels are commonly affected by localized forms of corrosion. In a gas sweetening plant, a plate type amine exchanger experienced a leakage of MDEA amine solution. The plates & other parts of exchanger were made from ASTM 304 stainless & ASTM A516 carbon steel. Sheet plates form one side was in contact with the lean amine solution, while the other sides with semi-lean amine solution. [30] During the investigation, it was revealed that intergranular corrosion was the damage mechanism of 304 stainless steels and cracking in the amine solutions being studied. No significant difference in the severity of intergranular corrosion and cracking between the lean amine and semi-lean amine solutions was there.it was identified that the main cause of corrosion in the 304 stainless steels within the amine exchanger unit was the degradation of the format anion to formic acid. It was also observed that the corrosion and cracking were more severe in the gasket region of the amine exchanger. This could be because of the localized corrosion in the gasket region as well as increased stress levels present under the gasket region. Overall, these conclusions highlighted that how much it is important to select the proper material during the design phase, when dealing with amine gas sweetening plants to alleviate corrosion and cracking issues in stainless steel components, particularly in areas prone to localized corrosion such as gasket regions.[30]

2.4 H_2S challenges presented to ESP systems:

In September 2011, Sikes et al [31]. conducted a study on the challenges of H_2S on downhole Electrical submersible pump system.

Hydrogen sulfide (H_2S) has the potential to significantly affect the reliability of electrical submersible pumping (ESP) systems through multiple mechanisms, including increased corrosion risk, formation of iron sulfide (FeS), and initiation of SS). H_2S is present in wellbores worldwide, and its presence can lead to several types of corrosion that target ESP systems, resulting in impulsive failure and production losses. ESPs have demonstrated suitability for wells with H_2S concentrations of up to 40%. Moreover, positive outcomes have been observed in wells with bottomhole temperatures (BHT) reaching 325°F and measurable levels of H_2S.[31]

With the reaction of H_2S and well bore fluid, free hydrogen is produced resulting in hydrogen embrittlement and with the passage of time, presence of free sulfur can lead to SSC in high – strength steels. Also (H_2SO_4) or free sulfur is formed with the reaction of H_2s with H_2O.

H_2S-resistant materials can be used in various configurations depending on the H_2S concentration and the BHT (Bottom hole temperature), allowing for the best combination of defense against the prevailing damage mechanism. corrosion-resistant couplings, fasteners, and housings and high strength shafting can be most protective against the corrosive elements of well bore. [31]

2.5 Inspecting Mechanical Properties and Corrosion Behavior of Rubber Packer in CO_2-H_2S Gas Wells:

In March 2021, Dong et al [32] conducted a study on the investigation of mechanical properties and corrosion behavior of rubber used in packers for CO_2-H_2S gas wells.

The corrosion behavior of rubber materials is of critical importance in packers under the corrosive co-existence environment of CO_2 – H_2S for ensuring the safe operation of oil and gas wells. The behavior of ALFAS®, FKM®, and HNBR® rubber under the co-existence environment of CO_2 & H_2S at elevated temperatures and pressures autoclaves was observed, and the mass growth rate, volume growth rate, and other mechanical properties of the samples were investigated. The corrosion mechanism of the rubbers was explored based on Energy Dispersive X Ray Spectroscopy (EDS) results and tensile fracture morphology. Results show that the mass and volume growth rate of ALFAS® rubber is comparable to FKM®, and growth is at a low rate, while sharp increases in mass and volume of HNBR® rubber are evident. Mechanical properties of ALFAS® and FKM® rubber are not affected by the corrosion, but significant effects were observed in HNBR®. FKM® rubber and ALFAS® have excellent corrosion and aging resistance properties, while HNBR® exhibits poor corrosion and aging resistance capabilities in the high corrosive environments of CO_2- H_2S. Therefore, the use of HNBR® rubber as a seal material as a packer seal material should be carefully considered under the CO_2-H_2S gas wells.[32]

In response to high rising demand of natural gas, high – acid gas wells have been drilled, the service environment of the wellbore is depicted by elevated temperature, high pressure, and high acidity. Excessive amounts of H_2S gas are frequently found in oil and gas fields, along with a small amount of CO_2 gas. These gases can severely corrode the tubing and downhole tools in the wellbore, causing leaks in the tubing and downhole, which jeopardizes the production and operational safety of the gas well. The packer is a crucial downhole tool that creates an isolation between the casing and the tubing to seal the annulus. Therefore, studying the characteristics of rubber materials in an H_2S-CO_2 environment is crucial to prevent corrosive media from entering the annulus between the oil pipe and production casing. However, after being damaged by H_2S and CO_2 gas, the packer's rubber is prone to aging, which furthers the seal failure. Major causes of seal failure in the packer are due to aging and blistering of rubber in HTHP environment. When a seal fails, CO_2 and H_2S gases leak into the annulus, creating constant annular pressure that can harm the environment and jeopardize the integrity of the wellbore.[32, 33]

Previous research has assessed the resistance of rubber materials to corrosion in a CO_2 atmosphere, but there are few reports of H_2S-CO_2 gas attacking rubber materials, making it challenging to provide guidance when choosing packers for H_2S-CO_2 wells. Therefore, understanding the corrosion behavior of packer rubbers in the presence of CO_2-H_2S is essential for ensuring the wellbore's safety. This study applied a high-temperature, high-pressure (HTHP) autoclave to expose the rubbers to a corrosive environment containing CO_2-H_2S. After conducting tests, the mass, volume, mechanical characteristics, and fracture morphology of the rubber were checked.[32]

2.6 Investigation on the H_2S-Resistant behaviors of acicular Ferrite and ultrafine Ferrite:

In January 2002, Zhao et al [34] investigated the H_2S-resistant behaviors of acicular ferrite and ultrafine ferrite.

The use of oil and gas pipeline steels is severely constrained by the presence of H_2S due to H_2S corrosion cracking. Sulfide stress cracking and hydrogen-induced cracking (HIC) are two of the most prevalent H_2S corrosion cracking issues for pipeline steels (SSC). In the past, numerous studies were conducted to improve the H_2S resistance of pipeline steels to prevent problems in the transport of oil and gas. The microstructure of the steel also has a role in its H_2S-resistant properties. [34]

Up till now, most of the research on the influence of microstructure on H_2S resistance has focused on microstructures such ferritic-pearlitic microstructure, upper/lower bainite, quenched martensite, and tempered martensite. The economic performance of the oil and gas industry depends on the proper choice of microstructure for pipeline steels. Mechanical characteristics play a key role in the choice, but pipeline steels in use's H_2S resistance also plays an important role.

Strict criteria for H_2S-resistant pipeline steels have been prompted by the tendency toward more extreme environmental conditions and higher operating pressure. The creation of microstructures with good mechanical characteristics and H_2S resistance is one of the manufacturers of pipeline steel's search objectives. Due to their comparatively high strength and toughness characteristics, both acicular ferrite and ultrafine ferrite have recently attracted the attention of steel makers. The two microstructures' H_2S-resistant nature, however, is not fully understood. [34]

The knowledge regarding H_2S-resistant behaviors of different microstructures, such as acicular ferrite and ultrafine ferrite, is primarily obtained through appropriate laboratory tests and practical experience in the field. In the past, traditional test procedures recommended by organizations like NACE International have been used as the basis for evaluating material performance in sour service applications.

In this study, both acicular ferrite and ultrafine ferrite were subjected to laboratory tests to assess their resistance to hydrogen-induced cracking (HIC) and sulfide stress cracking (SSC). The objective was to evaluate the H_2S-resistant behaviors of these two microstructures and determine which microstructure is the most suitable for oil and gas pipeline steels.

2.7 Effect of H_2S interaction with pre-strain on the mechanical properties of High-Strength X80 Steel:

In February 2016, Chen et al [26] conducted research on the influence of H_2S interaction with pre-strain on the mechanical properties of high-strength X80 steel.

The presence of hydrogen sulfide (H_2S) poses sizable challenges to use pipeline steel due to H_2S corrosion cracking damage mechanism. SSC and HIC are two common forms of H_2S corrosion cracking that affect pipeline steels. To develop the H_2S resistance of pipelines and ensure the safe transportation of oil and gas, extensive research has been conducted in this field. The microstructure of the steel plays a crucial role in deciding its H_2S-resistant properties. Previous studies have focused on microstructures such as ferritic-pearlitic, upper/lower bainite, quenched martensite, and tempered martensite.[26]

Economic performance of the oil and gas industry relies on selecting the appropriate microstructure for pipeline steels. While mechanical properties are crucial factors in the selection process, the H_2S resistance of pipeline steels also plays a significant role. The demand for H_2S-resistant pipeline steels has increased due to more challenging environmental conditions and higher operating pressures. Manufacturers of pipeline steels aim to develop microstructures that exhibit both excellent mechanical characteristics and H_2S resistance. [26]

Acquiring information about the relationship between microstructure and H_2S resistance involves scientific examinations and practical experience. Established test procedures, such as those suggested by NACE International [35], have been employed in laboratory evaluations of material performance for sour service applications. In this study, laboratory tests were conducted on acicular ferrite and ultrafine ferrite to assess their endurance to HIC and SSC. The objective was to evaluate the H_2S-resistant behaviors of these two microstructures and identify the most suitable microstructures for oil and gas pipeline steels. [36]

2.8 Electrochemical & SSCC behavior of tubing steels in H_2S/CO_2 annular environment:

In their research conducted in February 2017, Liu et al. [37] investigated the electrochemical and SSCC behaviors of tubing steels in a H_2S/CO_2 annular environment. The study aimed to understand the corrosion mechanisms and factors influencing SSCC in oil and gas wells where CO_2 and H_2S exist. Previous research primarily focused on internal corrosion of tubular and pipeline steels, while the corrosion occurring in the annular environment between tubing steel and casing steel received less attention. Several events of tubing steel failure in Chinese oil fields induced investigations, revealing that the accidents were caused by SSCC originating from the external surface of the tubing steel. The examinations of fracture characteristics, fractography, microscopic fractures, and surface films and deposits provided insights into the corrosion occurrence. The study emphasized the complexity of the low-temperature, high-pressure H_2S/CO_2, and low pH annular environment, which promotes higher sensitivity to SCC compared to high-temperature/high-pressure environments in down-hole wells. Due to limited information on tubing steel corrosion in annular environments, remarkably at high partial pressures of H_2S, designing control systems and selecting appropriate materials become challenging. Therefore, the investigation focused on comparing the corrosion behaviors of two commonly used tubing materials, 13Cr stainless steel and P110 steel, in the specific annular environment. This research findings helps to inform the material selection criteria, in oil and gas wells and the study helps to evaluate the impact of pH_2S on the corrosion behavior of tubular steels using static load u- bend immersion tests, electrochemical studies, and scanning electron microscopy (SEM).[37]

2.9 Investigation of pH_2S influence on 3% Cr Tubing steel corrosion behaviors in CO_2-H_2S-Cl_2 environment:

In their study conducted in 2015, Deng et al. [38] investigated the effect of pH_2S on the corrosion behaviors of 3% Cr tubing steel in a CO_2-H_2S-Cl^- environment.

The presence of CO_2 and H_2S can significantly affect the corrosion of transportation pipes, downhole tubing, and refinery facilities. Studies have shown that even minute levels of H_2S can delay general corrosion and pitting attack in carbon steel caused by CO_2 corrosion. This delay is ascribed to the establishment of a protective iron sulfide layer, particularly mackinawite, on the steel surface. The minimum H_2S concentration required to reduce CO_2 corrosion has been investigated, with calculations indicating that most previous studies were in the reduction zone, resulting in a reduced corrosion rate.

Localized corrosion, such as pitting attack, can occur in a sour environment due to factors like the cementite structure and galvanic coupling between FeS-covered and unprotected areas.

The CO_2/H_2S ratio has been a topic of discussion, with different thresholds proposed to define the corrosive environment. However, it is important to consider the absolute partial pressures of CO_2 and H_2S in the gas phase or the concentrations in the aqueous phase for corrosion studies. [38]

While earlier research primarily focused on carbon steel, this study targeted to examine the effect of H_2S on CO_2 corrosion in materials containing 3% Cr. By examining a wide range of studies on such materials, the study aimed to identify the critical point at which H_2S retards CO_2 corrosion. This information is crucial for understanding the corrosion behavior and selecting appropriate materials in sour environments.

2.10 Role of microstructure on the sulfide stress cracking of Oil and gas pipeline steels:

In May 2002, Zhao et al [39] conducted a study on the function of microstructure in SSC of oil and gas pipeline steels. Sulfide stress cracking is a significant concern in the said industry, as it can lead to disastrous failures of pipeline systems.

In the context of oil and gas pipelines, the occurrence of sulfide stress cracking (SSC) is a significant concern when exposed to aqueous hydrogen sulfide (H_2S) conditions. The choice of materials for pipeline construction is limited by the susceptibility to SSC. The industry expects pipeline steels with increased strength and improved SSC resistance to support the expansion of the oil and gas sector. [39]

Typically, there is a trade-off between SSC resistance and steel strength, where higher strength is often associated with lower SSC resistance. The yield strength or hardness of pipeline steels used in H_2S service is limited to 690 MPa or HRC22. However, efforts are underway to develop high-strength pipeline steels with valuable SSC resistance in sour gas environments.[40]

Chemical composition and microstructure are two key factors that can be adjusted during the steel production process to enhance SSC resistance. These factors are interconnected, and different thermo-mechanical control processes (TMCP) can result in varying microstructures for pipeline steels with a specific chemical composition. Currently, the two main types of pipeline steels being researched and used are ferritic-pearlitic steels and acicular ferrite steels. [39]

Acicular ferrite steels, characterized by an acicular ferrite matrix with a small amount of polygonal ferrite, are of unique interest due to their amalgamation of high strength and good toughness. Additionally, there has been growing interest in the ultrafine ferrite microstructure in recent years, as grain size can contribute to improved strength and fracture resistance. [39]

Previous research on the impact of microstructure on SSC resistance has focused on microstructures formed through traditional hot working or heat treatment processes, such as ferritic-pearlitic microstructures, upper/lower bainite, or quenched/tempered martensite. However, microstructures resulting from TMCP have been overlooked in understanding their SSC resistance. It is crucial to investigate how acicular ferrite-dominated microstructures and ultrafine ferrite microstructures, both beneficial for enhancing strength and toughness, contribute to SSC resistance. [39]

To develop high-strength pipeline steels with optimal SSC resistance, it is necessary to clarify the impact of microstructures created through TMCP. In a recent study, three microstructures, involving acicular ferrite-dominated, ultrafine ferrite, and ferritic-pearlitic microstructures, were assessed for SSC sensitivity using the bent-beam test. Microstructural analysis was conducted to examine the effects of these microstructures on SSC resistance. The findings from this study will be valuable for the commercial production of high-performance pipeline steels. [39]

2.11 Investigating the impact of heat treatment and microstructural transformations on API X-65 pipeline steel's susceptibility to HIC and corrosion in an H_2S environment:

In a study to analyze the sensitivity of an API X65 pipeline steel to hydrogen-induced cracking (HIC) and its corrosion performance in an environment containing hydrogen sulfide (H_2S) were investigated by Andijan et al. [40] in July 2021,. The study focused on the impact of heat treatment and the subsequent microstructural changes on these properties.

The API X65 pipeline steel is commonly used in the oil and gas industry, and its resistance to HIC and corrosion is of immense importance. Heat treatment is a widespread practice to enhance the mechanical properties and microstructure of steels. However, the effect of heat treatment on the susceptibility to HIC and corrosion in the presence of H_2S has not been extensively studied. [40, 41]

The study aimed to evaluate the existence of the API X65 steel to HIC and its corrosion functioning in an H_2S-containing environment under different heat treatment conditions. To examine and understand the influence of change in microstructure resulting from heat treatment were also examined along with the influence on material’s performance.

Annealing, normalizing, and quenching and tempering, were applied to the API X65 steel samples. These heat treatments induced different microstructural changes, including ferrite-pearlite, ferrite-bainite, and martensite structures.

The samples were then subjected to HIC testing to assess their susceptibility to cracking in a hydrogen environment. Corrosion tests were also performed to estimate the material's resistance to corrosion in the attendance of H_2S. Tests involved exposure to an acidic solution containing H_2S and monitoring the extent of corrosion and cracking. [41]

The findings of the study showed that the susceptibility of the API X65 steel to HIC and its corrosion performance were significantly influenced by the heat treatment and the resulting microstructural changes. Different microstructures exhibited varying levels of sensitivity to HIC and corrosion. [40]

The study provided insights into the relationship between heat treatment, microstructure, and the material's performance in H_2S-containing environments. This information can contribute to the development of optimized heat treatment processes for pipeline steels to enhance their resistance to hydrogen-induced cracking and corrosion, improving the reliability and safety of oil and gas transportation systems. [40]

2.12 Assessment of SSC in AISI 316L Stainless Steel under H_2S Environment during Service:

A study in an environment while in service was conducted in January 2014, by Attwood et al. [20] conducted a study on the occurrence of SSC attack on AISI 316L stainless steel.

A leakage was observed in a two-diameter pipe connected to a pressure safety valve in an acid flash gas compression facility in July 2011. Two other leakages in comparable lines on nearby compressors were detected over a two-day span. According to a root cause of failure analysis (RCFA), the leakages were caused by chloride-enhanced sulfide stress corrosion cracking. [42] A major contributing factor was assumed to be Summertime high ambient temperatures that cause discharge temperatures from the compressor after cooling to exceed 140º F. Cracking may have been accelerated by water cleaning of the discharge coolers, which led to brief (up to 2 h) temperature excursions up to 194º C, even though the defective pipes had been in service for four years. [20]

Three leaks were observed in two adjacent compressor trains' upstream pressure safety valve flare tail pipes over the course of two days (the failures took place in line Each failure happened at an elbow to pipe weld joints in a horizontal segment of the pipeline, with the leakages occurring in the (HAZ) of the weld and the upper section of the pipe. However, radiological evaluation was inconclusive. The initial in situ visual inspection revealed tiny pitting on the external surface. For metallographic analysis, all portions with failures were eliminated. [20]

2.13 Risk Assessment of Corrosion Under Insulation (CUI) on Industrial Piping:

Dr. Mark et al. presented a technical paper addressing the topic of Corrosion Under Insulation (CUI) and the associated risk it poses to industrial piping.[43]

The oil and gas industry faces a severe problem with corrosion under insulation (CUI) on industrial pipelines. Thermal and acoustic insulation materials are often subjected to several separate laboratory tests to determine their effects, but the applied system is extremely infrequently evaluated. Additionally, the evaluated physical values may not accurately reflect the potential impact that a particular insulation system or material may have on the risk of CUI (corrosion under insulation). A more comprehensive strategy is suggested that considers the CUI failure behavior, as well as the processes of water or water vapor ingress and retention, in addition to the applied insulating system. With this method, it is possible to undertake an individual risk assessment of the installed insulating systems against various water infiltration situations. [44, 45]. The configuration of the insulation system (e.g., insulation materials, Aluminum barrier foil, outer claddings), as well as the specified construction or installation methods, are additional influencing elements for the risk evaluation. The method suggested in this paper is projected to help the reader gain a better knowledge of insulation materials and how they affect CUI risk. It is also hoped that the reader will be better able to recognize vulnerable areas on the facility where CUI is likely to occur, enabling the development and implementation of appropriate CUI management strategies. Despite the prevalence and awareness of insulation materials, little study has been done on the best way to minimize CUI to maximize safety and prolong the life of the piping. [44]

CUI is a type of external corrosion that can be localized or widespread and is brought on by water or moisture that has become trapped on surfaces that have insulation covering them. The affected areas been not open or accessible for visual inspection therefore, the onset of corrosion cannot be detected, and in severe cases, serious corrosion with resultant compromise of system integrity might ensue. The onshore and offshore oil and gas sectors, as well as the petrochemical, specialty chemical, fertilizers, and allied industries, are all affected by the widespread problem of CUI, which affects thermally insulated equipment.

2.14 International codes and standards for H_2S corrosion analysis:

International codes and standards are designed on the best practices against H_2S. corrosion and help to guide the parameters affecting H_2S in any plant equipment, their corrosion rates, their partial pressure, impact of temperature and pH in any electrolyte. These codes and standards also guide the possibility of failure of any equipment in H_2S environments and the consequences of the failure of that equipment.

2.14.1 National Association of corrosion Engineers (NACE):

i) NACE MR0175/ISO 15156: This standard provides requirements and recommendations for materials selection and corrosion control in environments containing H_2S in oil and gas production, drilling, and related operations. [7]

ii) NACE SP0108-2008: This standard gives guidelines for corrosion control of H_2S service in oil and gas production systems.[17]

2.14.2 American Petroleum Institute (API):

i) API RP 571: This recommended practice provides information on damage mechanisms and material selection for various industries, including oil and gas, and covers H_2S corrosion extensively. [13]

ii) API RP 939-C: This document focuses on avoiding sulfide stress corrosion cracking (SSC) in carbon and low-alloy steels used in the refining and chemical processing industries.

2.14.3 American society for testing of materials ASTM International:

i) ASTM G161: This standard provides a guideline for conducting laboratory tests to evaluate materials for resistance to sulfide stress cracking in a specific H_2S environment. [4]

ii) ASTM G185: This standard outlines the procedures for conducting atmospheric corrosion tests in H_2S-saturated air or other corrosive environments. [4]

The above-mentioned codes and standards are in normal practices of E & P and refinery industries.

2.15 Key Factors H_2S corrosion

After thorough review of guidelines set by international codes and standards the following factors have been identified as key factors influencing H_2S corrosion.

2.15.1 Impact of pH on H_2S corrosion:

pH <2: Iron sulfide deposition is unlikely to occur, but it can speed up the process of iron dissolution. [5]

3<pH5: The formation of FeS scale, which acts as a corrosion inhibitor, complicates the corrosion process when reacting with H_2S. Figure 11 illustrates the concentration of H_2S in the air in parts per million (PPM) and the associated short-term and immediate dangers to personnel and workers. The resulting product of this reaction can contribute to additional corrosion. Although temperature may not have a significant impact on H_2S corrosion, higher temperatures can promote the conversion of sulfide into elemental sulfur. It is worth noting that the oxidation of sulfide with any oxidant can generate elemental sulfur, as mentioned previously.

$$H_2S + O_2 = S + 2H_2O$$

In a moist environment, iron sulfide scale is formed through the reaction of elemental sulfur with iron. Field experiences have demonstrated that sulfur is extremely aggressive towards metals, particularly in terms of pitting corrosion, stress corrosion, and general corrosion. This highlights the damaging effects that sulfur can have on metal surfaces, leading to various forms of corrosion. Proper measures and corrosion mitigation strategies should be implemented to protect against the detrimental impact of sulfur on metal structures.

2.15.2 Impact of Partial Pressure & Concentration on H_2S Corrosion:

Partial pressure and concentration of H_2S plays a key role in H_2S corrosion and is directly proportional to the concentration of H_2S in PPMs and partial pressure of H_2S inside any vessel, flow line, down hole tubing & casings. High temperature, Partial pressure of H_2S more than 0.05 Psi and concentration of H_2s more than 50 PPMs in any electrolyte will accelerate H_2S corrosion and studies have revealed that up to 50 PPMs of H_2S concentration, a protective layer is formed and remains protective up to 50 PPMS, however exceeding this limit, the hydrogen sulfide layer is broken, and material is exposed to H_2S Corrosion.[5]

2.15.3 Impact of Temperature:

Temperature plays a vital role in acceleration corrosion process, with the increase in temperature, the reactivity of hydrogen sulfide also enhances, making H_2S more corrosive. As a result, corrosion rate increases with rising temperature when metal is exposed to H_2S environment. [46]

2.15.4 Sweet spot:

The threshold temperature above which H_2S corrosion becomes more severe is termed as "sweet spot" for H_2S corrosion. Typically for carbon steel, around 140 º - 194 º F is the threshold temperature. Below this threshold temperature (sweet spot), the rate of corrosion is low. But once the threshold temperature is surpassed, it increases significantly. The mentioned type of corrosion mechanism involves absorption of atomic hydrogen by the metal which leads to cracking and subsequent failure under stress. Hydrogen induced cracking (HIC) and sulfide stress cracking (SSC) in metals exposed to H_2S environment is promoted at elevated temperature. The risk of HIC & SSC at evaluated temperatures is particularly higher.[5]

2.15.5 Impact of Hardness of H_2S Corrosion:

Hardness can have a significant impact on H_2S corrosion. The hardness of a material refers to its resistance to deformation, particularly indentation or scratching. Here are some key impacts of hardness on H_2S corrosion:

2.15.6 Increased susceptibility to corrosion:

Hardness is inversely related to a material's resistance to corrosion. In general, harder materials are more susceptible to corrosion, including H_2S corrosion. This is because harder materials often have lower corrosion resistance and are more prone to microstructural defects and stress concentrations, which can facilitate the beginning and propagation of corrosion.[5]

2.15.7 Stress corrosion cracking (SCC):

Hardness plays a role in the susceptibility to stress corrosion cracking (SCC) in the presence of H_2S. SCC is a type of corrosion that occurs under the simultaneous influence of tensile stress and a corrosive environment. Harder materials, particularly high-strength alloys, are more susceptible to SCC in H_2S environments due to their reduced ductility and increased sensitivity to hydrogen embrittlement.

2.15.8 Hardness-induced cracking:

High hardness levels can promote the formation of cracks in metals exposed to H_2S environments. Hardness-induced cracking can occur due to several factors, including hydrogen embrittlement and environmentally assisted cracking. The combination of high hardness and the presence of hydrogen sulfide can increase the likelihood of crack initiation and propagation.[5]

2.15.9 Impact of H_2S to Human life and Equipment:

H_2S Toxic Dispersion reported for the following Concentrations :[1]

I. 5 ppm STEL (Short term exposure limit) as per NIOSH

II. 10 ppm REL (Recommended exposure limit) as per NIOSH/OSHA Permissible Exposure Limit (PEL) Limit

III. 30 ppm criteria for Muster Point

IV. 76 ppm AEGL -3 (10 minutes) AEGL guidelines for population outside, Acute exposure guideline levels (AEGLs) provide information about how harmful airborne chemicals can be to humans in a situation where they are exposed to them only once in their lifetime or on rare occasions.

V. 100 ppm (IDLH) “Immediately Dangerous to Life or Health value as per NIOSH

VI. 700 ppm Death within 40-minute s as per NIOSH/OSHA guidelines

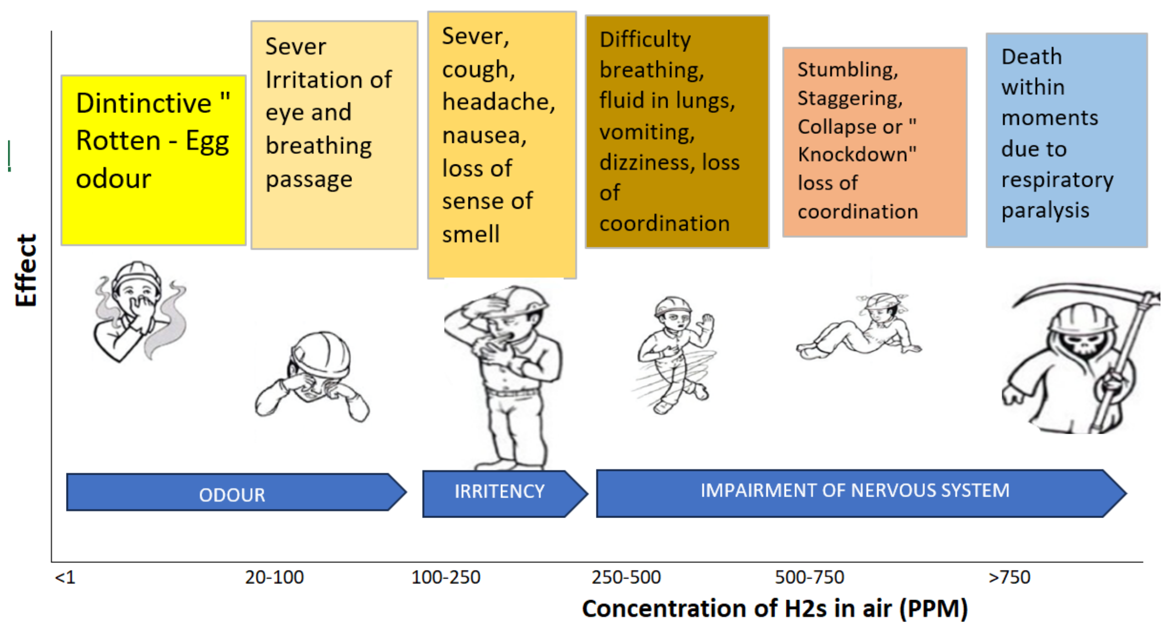

Figure 18. Concentration of H2S in air PPM & its short term & immediate danger to human life

Chapter 3:

3 Experimental Work

This chapter highlights the experimental and inspection techniques used for the health and mechanical integrity of Regeneration Gas heating and cooling systems in the environment of H_2S around 50 parts per million (PPMs) and containing hydrocarbons and water and other impurities. [5]

The experimental work was carried out under the guidelines of American Petroleum industry (API) 510 & 570 in which the equipment was inspected internally and externally to find damages / flaws / defects or any recordable findings for future monitoring to ensure equipment's' integrity against the un-expected entry of 50 PPMs H_2S for future use up to next ATA (Annul Turn Around) or up to next inspection interval. [5]

The insulated heat exchanger was inspected externally and internally by dropping the channel head, pulling bundle out placed at ground for inspection. Pre & post clean inspection was conducted for Channel Head, Shell, and tube bundle. The external condition of shell and Paint/coat condition observed as observed from insulation pockets. Saddle supports and anchor nuts.

Tube ID& OD (Internal diameter & outer diameter) during pre-clean inspection. Post clean inspection was done and found some minor rusting inside shell and tube sheet, tube ID. Channel and its cover GSS were found satisfactory. Baffle plates, impingement plate and tie rod lock nuts were visually inspected. Associated nozzles N2, N4 for channel were found with some minor rusting on the inside surface. Inlet/Outlet nozzles N1, N3 flanges for shell were not opened for inspection. One NUT was found inside shell body which was removed. Tube ID to the extent observed were free from choking. Tube sheet condition found satisfactory. TTS (tube to tube sheet) weld joints were found visually acceptable. RFT (Remote field testing), ECT (Eddy Current Testing) was conducted for 102 (40%) out of 256 total tubes.

3.1 Methodology:

The regeneration gas cooling and heating system was inspected internally as well as externally to evaluate any internal or external defects as detailed below.

The following techniques were used to conduct an internal inspection of the equipment.

1. Internal & visual Inspection
2. Eddy Current / RFT testing of Tubes.

To conduct inspection, analyze any damage, metal loss, or surface / sub surface and any changes in the microstructure of the equipment, and assess the integrity of the regeneration gas cooling and heating system following nondestructive inspection techniques were used. [3]

1. Dye Penetrant Inspection
2. Magnetic Particle Inspection
3. Ultrasonic Flaw Detection
4. Ultrasonic thickness gauging inspection
5. Hardness testing
6. Metallography / Replica

3.2 Internal Inspection:

Internal inspection was offered with limited access through opening. The Internal inspection was conducted by dropping the channel head, pulling bundles out placed at ground for inspection. Pre & post clean inspection was conducted for Channel Head, Shell, and tube bundle. The internal inspection was conducted to observe any internal cracks, scattered pits, clusters of pits, scaling or rusting on the internal surface of the equipment. The light torch and borescope / snake eye inspection tool was used to examine the areas which were not accessible by naked eye. Pit gauge was used to calculate any pit or cluster of pits. Proper ventilation and passage of air was managed through exhaust fan. All the abnormalities / anomalies were recorded.

3.3 Visual inspection:

Visual inspection was conducted to observe any obvious anomalies, metal loss, surface cracks, scattered pits, or cluster of pits on the surface of regeneration gas cooling and heating system. The equipment was first made clean with the help of wire brush to remove any scale, debris, dust, or any other containments. This visual inspection was aided by torch light, and borescope. Borescope is a flexible optical device which is equipped with a camera that helps to inspect the narrow and inaccessible locations of any equipment. All the areas which were not accessible by naked eyes were approached and examined through borescope. The accumulation of scale, rust / metal deteriorations were recorded and noted and were made part of the complete inspection.

3.4 Eddy current testing / Remote field testing (RFT):

Since the regeneration heating and cooling system consists of shell and tube and the tubes are the delicate and most important components of said system, and health & mechanical integrity assessment is very important, it was carried out through Eddy current / RFT technique, the tubes were cleaned and tube bundles were taken out from the shell with the help of heavy crane and were placed on the ground for their internal inspection with the help of RFT NDT technique. [23]

The remote field-testing equipment was calibrated with the available calibration block and the numbering of tube bundle was conducted to locate / trace any defects observed during inspection and testing. Figure 23 shows the numbering conducted in tube bundles. The inspection procedure adopted for this technique is under ASME Sec V.

The material of tube was SA-179 with outer diameter of 19.05mm, wall thickness recorded was 2.11 mm, length of each tube was 4000 mm, with total no of tube 256 and 102 no of tubes were inspection. The model of tool used for the inspection was M-5800 with serial no: 819536-01 and probe type was single exciter. The calibration of the probe was conducted prior to inspection of tube bundles to ensure the accuracy of the testing. Internal and external cleaning of tube bundle was conducted through the water flashing and after the confirmation of cleaning procedure, marking of each tube in the tube bundle is marked to ensure and confirm the back tracing of inspection report. [23]

Figure 19. Flushing for removal of dirt through water jetting

Remote field-testing equipment consists of a wire like tube connected with a device. The wire of RFT tool was inserted in each tube of the equipment and a low frequency pulsed magnetic field was generated to inspect and evaluate each of the tubes to access any metal loss. It makes use of transmitter coils to produce a magnetic field that passes through and out of the tube wall before returning to the tube to strike the reception coil. Equal detection sensitivity at the inner and outer surfaces of the tube is possible with this technique. While tube thinning can be detected using the absolute mode, the differential mode of Remote Field Testing provides for more accurate fault detection (corrosion, erosion) The generation and decay of eddy current is reliant on the thickness of the material and the position of opposite edge (black wall) and these factors strongly influence the decay and generation function of eddy current. Figure 22 & Figure 21 above show the tube bundles and the evidence of numbering tubes inside the bundles. Average thickness of the material was measured from the strength of the eddy current, and the time taken for each variation. Specific algorithm and calculations for lift off and wall thickness available in the attached software was used to calculate the average wall thickness with the help of absolute mode of RET equipment. Corrosion and erosion detection in the tube was also inspected with the help of available RFT equipment. [13]

Figure 20. Inspection of tube through RFT and numbering of tubes

External inspection:

3.5 Dye Penetrant Inspection:

Dye penetration testing was conducted by cleaning the surface and removing any dust or debris to observe any surface cracks with the help of visible solvent cleaner as per guidelines of ASME Sec V & acceptance code of ASME section VIII Div I [47] for the partition plate of regeneration gas cooling and heating system.[47]

To assess any surface cracks on equipment, dye penetrant inspection was conducted in the following sequence.

3.5.1 Surface Preparation for Dye penetration:

Surface preparation is a critical step in the dye penetration testing process to ensure accurate and reliable results. The following are some general steps for surface preparation for dye penetration testing:

3.5.2 Clean the surface:

The surface to be examined must be clean and free of any dirt, grease, oil, or other contaminants that may affect the test results. Clean the surface with a suitable solvent such as acetone, isopropyl alcohol, or another cleaner that is appropriate for the material being evaluated.

3.5.3 Dry the surface:

After cleaning the surface, ensure it is completely dry before starting the test. Any residual moisture can affect the test results, so it is essential to use a clean, dry cloth or air blower to dry the surface.

3.5.4 Surface Roughness:

The surface roughness was ensured by removing paint / coat or any containment and dust over the surface of the equipment. This was done to remove any blockage or hurdle that could restrict or block the penetration of dye in the surface / or surface defects. roughness of the surface was done using a wire brush and sandpaper. The appropriate surface roughness was ensured for the material being evaluated. Being critical equipment, it was ensured no damage was done to the surface of equipment during wire brush and scrapper being used.

3.5.5 Application of dye:

Once the surface had been prepared, dye penetrant was applied to the surface, ensuring that it completely covered the area to be evaluated. The dye was allowed to penetrate the surface for any available potential defect on the surface up to the curing time of dye.

3.5.6 Removal of excess dye:

After the dye had been allowed to penetrate, excess dye from the surface was removed using clean, dry cloth or paper towel.

3.5.7 Application of developer:

Applied the developer to the surface and allowed it to dry for the recommended time. The developer draws the dye out of any surface defects, making them visible to the naked eye.

3.5.8 Inspection of the surface for defects:

After the developer had dried, inspected the surface for any visible indications of surface defects. Any defects found were carefully evaluated to determine their size, shape, location, and potential impact on the component's performance.

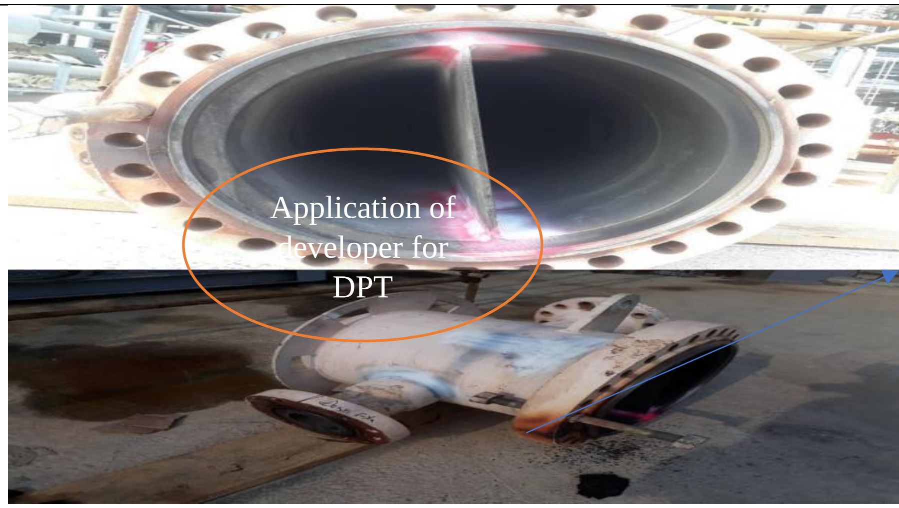

Figure 21. Dye penetrant testing of partition plate

3.6 Magnetic particle inspection:

MPI was conducted as a non-destructive testing technique to identify any potential threat at the surface and near surface of nozzles and Tee joints of the regeneration gas cooling and heating system. Magnetic particle inspection was conducted under the guidance of ASME section V and acceptance criteria ASME Sec VIII Div I, components that were inspected thought this technique are inspection including nozzles and Tee joints to detect any surface anomalies in the weld joints and Tee joints.

The following steps were followed to conduct the magnetic particle inspection.

3.6.1 Surface Preparation for Magnetic particle inspection:

Surface preparation was conducted to ensure that the area of interest to be inspected is clean and free from magnetic material as the presence of said material can create interference with the inspection tool.

3.6.2 Identification of suspected defects:

As the surface and sub surface defects were to be identified, the appropriate magnetic particle technique was utilized and that was use of fluorescent technology and for that magnetic particle bath of mixture was prepared.

3.6.3 Pre-cleaning of Surface:

Surface was cleaned to eliminate dirt, oil, paint, or other impurities that could affect during inspection and for that purpose cleaning, degreasing and surface cleaning was conducted with the help of power brush.

3.6.4 Magnetization of surface:

Magnetization of surface was conducted by applying magnetic field using central conductor.

3.6.5 Inspection of Surface:

Inspection of surface was conducted after application of magnetic field to analyze the indications (defects) and irrelevant indications which could be because of surface roughness.

3.6.6 Post-inspection cleaning:

Surface of regeneration gas cooling and heating system was cleaned, and magnetic particles were removed with the help of cleaners and wire brush.

Figure 22. MPI inspection

3.7 Ultrasonic flaw detection:

A nondestructive technique used to identify any potential threat on welding joints, heat affected zone and the base metal of the any asset is Ultrasonic flaw detection.

Ultrasonic flaw detection was carried out under the guidance of ASME section VIII, Div I to assess the health and integrity of weld joints at different angles with the help of UFD probe and no significant weld defects were observed and were found acceptable under the acceptance code of ASME section V, article IV and ASME section VIII, div 1.and acceptance code is API – 570 , NDE procedure was EPP/PAK/PR-NDT-03, Test Equipment. [13]

This inspection technique was conducted using the following procedure.

3.7.1 Ultrasonic flaw detection setup:

Ultrasonic flaw detection equipment setup was made ensuring that the transducer is properly connected, and the calibration of equipment / tools was conducted with the help of available standard calibration block.

3.7.2 Selection of Couplant:

As ultrasound needs a medium to travel through the surface of material to be evaluated / inspected therefore usage of proper Couplant is essential. For this purpose, gel was used as a Couplant to ensure good ultrasonic coupling between transducer and the weld joints.

3.7.3 Adjustment of instrument:

Adjustment of instrument was conducted to adjust the sensitivity of signal and response with the help of gain and range option available in the instrument.

3.7.4 Scanning of the weld joints:

Scanning of the weld joints was conducted with the help of instrument probe at different angles to detect any flaw, defect, or any anomalies in the weld joints, base metal and the area which is affected by heat during welding. Transducer was placed on the surface of the weld joints, base metal and heat affected zone to scan for the defects. During the scanning process of the above-mentioned areas, the indications such as echo, back- reflections and change in amplitude were carefully observed. Such kinds of indications come from any available defects on the inspected area. The indications observed during inspection were carefully analyzed and their nature, size, and location of any detected flaws or discontinuities were finalized. [6]

Figure 23. Application of Ultrasonic flow detection

3.8 Ultrasonic thickness gauging:

Ultrasonic thickness gauging was conducted with the help of thickness gauging meter and the equipment is shown in figure 16. Ultrasonic thickness gauging was conducted with the help of portable and recordable thickness gauging meter which was calibrated with the help of calibration block and thickness / condition measuring locations were at clock positions of shell, dish end and nozzles of the Regeneration gas cooling and heating system with the help of Gel which was used a Couplant. The thickness gauging procedure was conducted under the guidance of ASME sec V with UTG procedure NO: EPP/PAK/PR-NDT-03, the calibration block used was step wedge. [3, 4, 22]

Ultrasonic thickness gauging was conducted at the shell of the regeneration gas cooling and heating systems to access the uniform metal loss in the guideline of EPP/PAK/PR-NDT-03 procedure. And ASME Section V. [47, 48]

The following essential steps were followed to conduct thickness gauging survey.

3.8.1 Selection of Thickness / condition monitoring location:

Thickness / condition monitoring location (TMLs / CMLs) plays a vital role in thickness survey. During the thickness survey TMLs / CMLs were carefully selected under the guidance of API 510 and ASME section VIII Div 1 code. The bottom of the shell was selected as water (electrolyte) being heavier than gas and crude travels at the bottom side of the shell of regeneration gas cooling and heating system. Metal loss, pit(s) in the forms of cluster or in scattered forms can be expected inside the bottom surface which. Can be a potential threat to the surface of equipment. TML / CMLs marking with help of permanent marker was conducted at the shell, dish ends and attached nozzles of the equipment. To trace back the any anomaly found during thickness survey, the isometric of TMLs / CMLs was sketched. Figure no.34 in the appendix – 1 shows the detailed marking of all thickness / condition monitoring points.

3.8.2 Calibration of Thickness meter:

To conduct thickness survey, it is important to calibrate the thickness gauging meter with the help of an available calibration block. Calibration of the thickness meter was conducted with the help of solid calibration block.

3.8.3 Selection of Couplant:

Gel and water are used as a Couplant during thickness survey of any equipment, assets, or any pipeline. However, gel was selected to be used as a Couplant for the thickness survey as the gel can adhere to the surface of the equipment and can provide vacuum for the traveling of waves from UT meter to the surface of equipment.

3.8.4 Placement of Thickness meter probe:

Probe is a device which relates to the UT meter to check the thickness of any conductive material ranging from varied sizes, temperature ranges and different angles to conduct UT thickness survey. Appropriately selected probe was placed on the surface of equipment with gel as a Couplant.

3.8.5 Measurement of thickness:

Active ultrasonic thickness meter and after selecting the appropriate setting of meter (Density, sound velocity and probe frequency), the probe was placed perpendicular to the surface of equipment making sure that the contact between the probe and surface is accurate and thickness reading was noted down. For every TMLs / CMLs, four reading at o clock positions were taken and recorded in the UT meter which were then retrieved from the meter through data cable. [3]

Figure 24. Application of Thickness gauging by applying gel as Couplant

3.9 Hardness testing:

Hardness testing of base metal, weld joints and HAZ area were conducted with the help of portable hardness tester and the recorded readings were noted down and analyses under the guidance of NACE MR 0103/ MR 0175 & ASTM-E10-15 & ASTM E10-15. [49]

It involves the following steps:

3.9.1 Sample Preparation:

The area of interest was selected, and cleaning of the surface was conducted to remove any foreign material I-e dirt, debris of any other containments. The cleaning of surface was conducted with the help of degreaser, and WD-40. Sample / areas selected for the hardness testing were base metals, weld joints, and HAZ (Heat affected zones) as it is considered that these areas most suitable and favorite for H_2S corrosion.

3.9.2 Calibration and setup of Hardness tester:

The hardness tester was calibrated with the help of available calibration and the necessary setting of hardness testing was set before the start of hardness testing inspection.

3.9.3 Placement of Hardness tester:

After calibration of hardness tester and setup of the hardness testing equipment, tester was placed perpendicularly at the already selected condition monitoring locations the base metal, weld joints and HAZ and reading was noted and recorded in the available memory of tester equipment.

Figure 25. Application of hardness testing through portable hardness tester

3.10 On-site Metallography:

Replica metallography is a technique used to study the microstructure of materials by creating a replica or copy of the surface features. The metallography / Replica was conducted under the guideline of ASTM E3, which guides / instructs for the preparation of specimen preparation, cutting, grinding, mounting of sample, polishing, and etching of the sample.

3.10.1 Sample selection:

To understand any change in microstructure at elevated temperatures and due to the presence of H_2S in fluid, base metal, weld joints and HAZ areas were selected for the metallography technique.

3.10.2 Sample Preparation:

Surface to be replicated was cleaned enough that it was free from dirt, grease, or any. Six different points during visual inspection were selected for the metallography of the fitting material along where change in direction of flow of fluid was expected. These points were elbow areas of regeneration gas cooling and heating system and base metal along with weld joints and HAZ areas were identified during visual inspection for in-situ metallography by the portable metallography.

i) The sample spot was first grind with emery paper starting from 80 to 3000.
ii) Diamond paste was applied at the sample spot area after the confirmation of proper grinding.
iii) 3 % Nital was used as an etchant during the in- situ metallography.

iv) A portable microscope was placed perpendicular to the area of interest and the image was recorded.

(a)

(b)

(c)

Figure 26. (a) Grinding & polishing of spot area, (b) Diamond paste & Etchant (c) In-situ Metallography of Regeneration Gas cooling & Heating system.

3.10.3 Microscopic examination by portable Microscope:

The portable microscope was properly assembled and calibrated with the calibration block before positioning the microscope. The microscope was placed on clean, well grinded, and etched spot area of the component and focus was adjusted and lighting was set to achieve the clear image.

To visualize the image, necessary adjustments were done. The image was captured through the attached digital camera after optimizing the image quality. Six shots for each component were taken and recorded.

3.11 Overall inspection pictorial display:

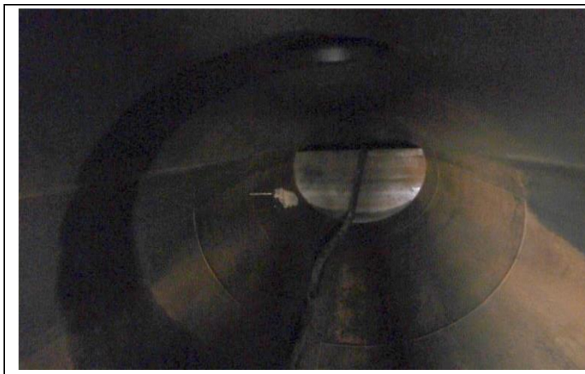	
(a)	(b)
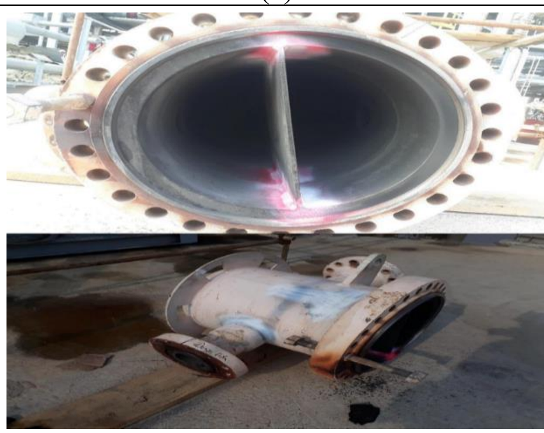	
(c)	(d)
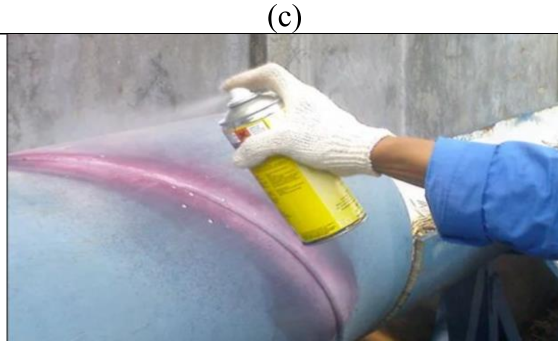	
(e)	(f)

Below pictures show the overall inspection conducted on regeneration gas cooling and heating system of an E & P company for health and integrity. assessment.

Figure 27. (a) Overall view & Saddle support condition of heat exchanger and (b) Name plate with specifications of regeneration system (c) Dye Penetration testing of equipment (d) Insulation pocket for inspection (e) Tube bundle inspection (f) Numbering of tube bundle

Chapter 4:

4 Results & Discussions

Comprehensive set of inspection techniques was conducted that can effectively assess the integrity and health of the Regeneration gas cooling and heating system installed in an Oil and Gas plant under the guidelines of industrial codes and standards and to which inspection / non-destructive technique is helpful to assess the health and integrity of candidate equipment. The focus of the inspection is to identify and evaluate surface and sub-surface defects, as well as detect any metal loss that may occur during the intervention process involving around 50 parts per million (PPMs) of H_2S. Furthermore, the inspection aims to contribute to the optimal functioning of the equipment, including its components such as tubes and shells, which operate within a temperature range of 400-600^o F and a working pressure of 1625 psi. The material of construction for the equipment is specified as SA-516 Gr-70, and the manufacturing date is noted as 2016. As a result of inspection, internal and external inspection, calculation to be conducted to evaluate the remaining life, any area which can be prone to SSC in H_2S environment having elevated temperature and pressure and based on the inspection findings and results under the guidance of ASME standards, API relevant standards corrective actions to be taken.

Calculations are conducted because of inspection techniques mentioned in Chapter No.3.

4.1 Visual inspection :

Visual inspection of regeneration gas cooling and heating system was conducted in the light of guidelines of API-510. During visual inspection, hard scale was observed on the internal surface of the equipment which could be because of elevated temperature which is evident in the design and flowing parameters of the said equipment. This hard scale was removed by cleaning with water. Accumulation of black sludge was observed over the external surface tube bundle, which was professionally cleaned by water jetting, source of this sludge is crude oil. Figure 28 (d) shows the post and pre cleaning conditions of tube bundle.

During visual inspection, location for inspection point of dye penetrant testing, Magnetic particle inspection, ultrasonic flaw detection, thickness gauging point, hardness testing locations and replica points were marked. insulation material and its integrity were conducted visually. Also, the insulation pocket for inspection to be conducted was also marked. During visual inspection, any sign, or susceptible areas where corrosion under insulation can occur were carefully checked, however no signs were observed by this inspection technique.

All the bolts, gaskets and saddle support were observed and inspected visually, and found in good condition with no sign of external or internal corrosion.

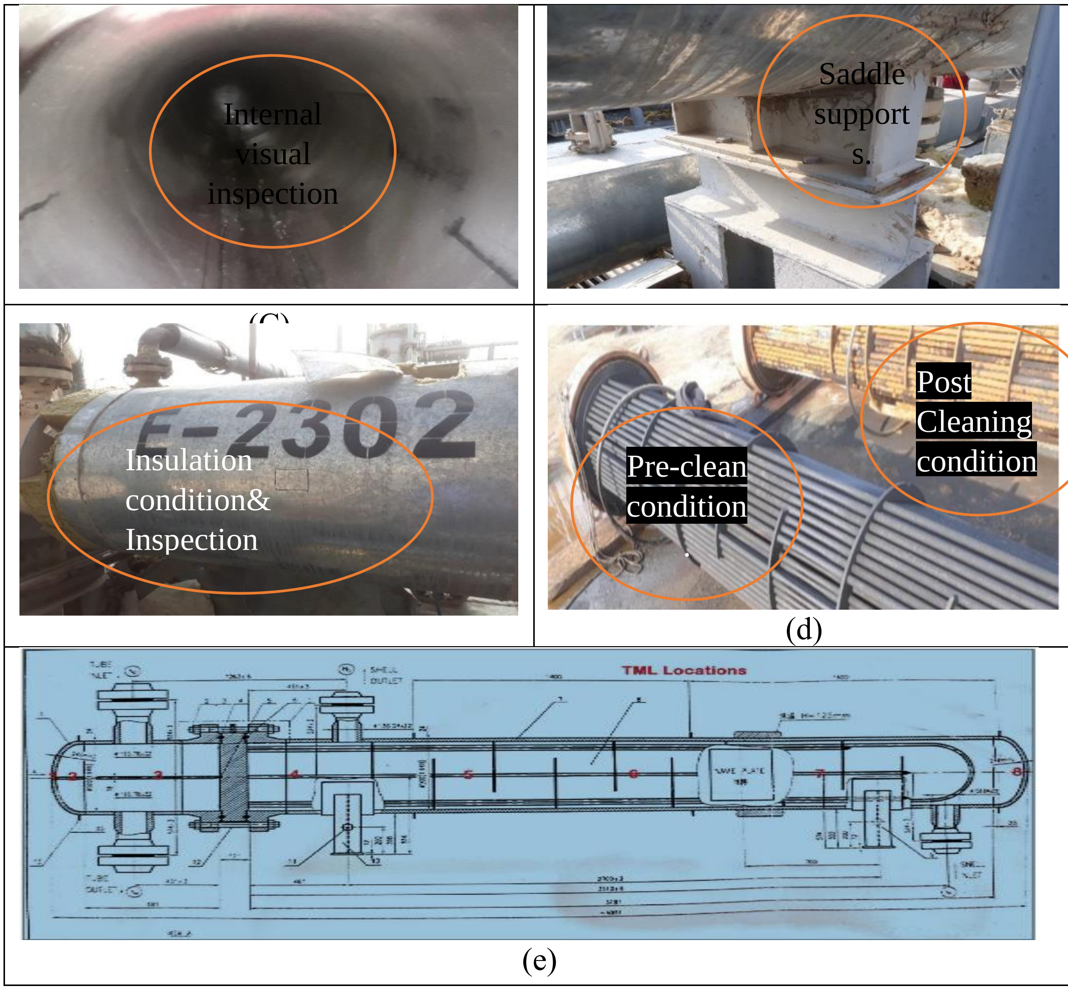

Figure 28. (a) Internal visual inspection, (b) External Visual Inspection, (c) Inspection condition of Insulation material, (d) Pre-& Post cleaning condition of tube bundles, and (e) Inspection measuring locations.

The overall condition of regeneration gas cooling and heating after internal & external visual inspection is satisfactory.

4.2 Remote Field Testing of tubes:

The remote field-testing results of tube bundles, conducted after adopting procedures as mentioned in chapter 3 of this thesis, results of each tube with metal loss in mm and in percentage were recorded. Total 256 tubes are in tube bundle and 102 tubes were selected after visual inspection, original thickness of each tube 2.11mm, outer diameter 19.05 mm and length of each tube 4000mm, with tube material SA-179 after conducting remote field testing of tubes, 02 tubes were found corroded with metal loss of less than 20 percent of their total thickness. The recorded thickness of corroded tubes is higher than the minimum required thickness as calculated in table NO. under the ASME section v.

RFT ECT was conducted for 102 (40%) out of 256 total tubes. NDT techniques successfully performed as per available access and results found satisfactory and the results are shown in the tables 11, 12 & 13 and figure 25 shows the pictorial display of tube bundle defects. [50]

Table 1 Remote field testing of tubes and table 9 & 10 shows the percentage metal loss of tubes observed during inspection.

Table 2. Type of defects in tube bundle

Defect Range	**Number of tubes:**	**Inspected (%)**
No Defect (NDD)	100	98.0%
0% < Defect <= 20%	2	2.0%
20% < Defect <= 40%	0	0.00%
40% < Defect <= 60%	0	0.00%
60% < Defect <= 80%	0	0.00%
80 % < Defect <= 100%	0	0.00%
Defect Type	**Number of tubes:**	**Inspected (%)**
No Defect (NDD)	100	98.0%
Pitting (PIT)	0	0.00%
Wall Loss (WLS)	2	2.0%
Restricted (Rs)	0	0.00%
Plugged (Plug)	0	0.00%

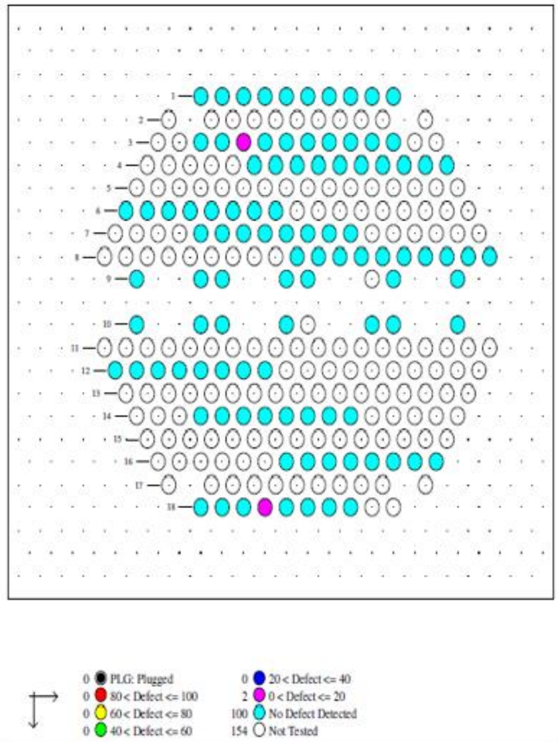

Figure 29. Pictorial display of defects of tube bundle.

4.3 Dye Penetrant Inspection:

Dye penetrant inspection reveals the surface cracks. Partition plate of regeneration gas cooling and heating system inspected with DPT inspection results were carefully observed and if there is any trapped penetrant in the crack or defects was given sufficient time to migrate to surface as per guidelines of AMSE section V div however no such dye penetrant was observed which could be entrapped in the crack or defect and no sign or indication was observed during this inspection technique. Partition plate is found without any surface defects and is safe to operate at current operating parameters. Figure 31 shows the dye penetrant testing applied on the partition plate and table 3 shows the acceptable & satisfactory test results as per above mentioned inspection code and standards.

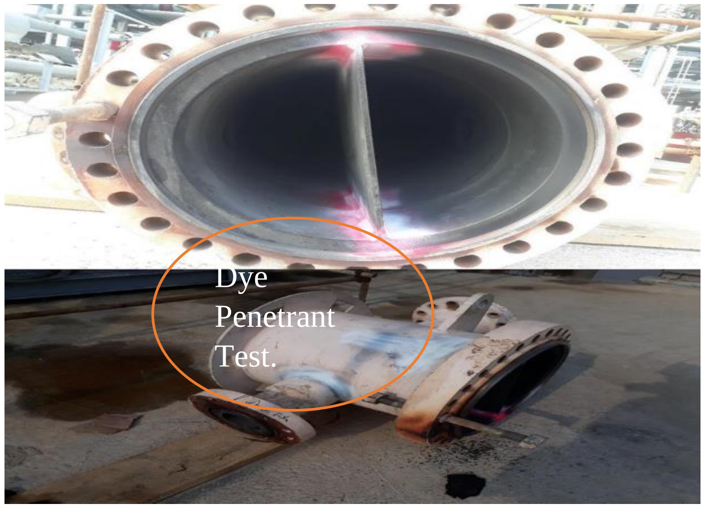

Figure 30. Dye penetration testing of partition plate

The table below shows the inspection conducted through MPI inspection technique for the channel head cover partition plate, which is a critical component of regeneration gas cooling and heating system.

Table 3. Dye Penetrant Inspection

S. No	Description	Quantity	Inspected Area	Result
1	Channel Head Cover - Partition Plate	100%	Partition Plate Weld	Acceptable

Dye penetrant conducted on the partition plate of the equipment was carefully examined and dwell time was given to soak inside the material and developer of the dye penetrant test to ingress inside any flaw, however after careful examination no flaw, no defect revealed, and the partition plate is safe to operate.

4.4 Magnetic particle inspection:

MPI of Tee joints and nozzles carried for shell, channel head cover and all the areas of said components were inspected 100 %,. The surface of the magnetized components was inspected and was examined very carefully with the help of visible light for any indication of defects, flaws, or any anomalies. The indication appears in the form of particle accumulation which appears as distinct line, cluster, or patterns on the surface of these components. However, after carefully observing the surface of Nozzles & Tee joints of Regeneration gas cooling and heating system with the help of appropriate lighting source, no indication was observed during the inspection and the health and integrity of inspected components is found satisfactory and is safe to operate at current flowing conditions. The results show temperature, partial pressure of H_2S has not damaged the surface of nozzles and Tee joints and the results are acceptable under the ASME section V div 1.

Table 4. Magnetic particle inspection results

Sr. No.	**Description**	**Result**
1	Nozzle-1 (Tube Outlet)	Acceptable
2	Nozzle-2 (Tube Outlet)	Acceptable
3	Nozzle-3 (Tube Outlet)	Acceptable[51]
4	Nozzle-4 (Tube Outlet)	Acceptable
5	Tee Joint-2	Acceptable
6	Tee Joint-2	Acceptable

Magnetic particle inspection conducted on the nozzle-1, nozzle-2, nozzle- 3, and nozzle -4 along with tee joints, ample time was given for magnetization and the surface was examined through ultraviolet light to observe any defect or flaws on the surface or sub-surface. No anomalies, flaws, or defects observed.

4.5 Ultrasonic flaw examination:

. UFD carried out the welding joints of Regeneration gas cooling and heating system of E & P company and sound waves were generated to encounter any flows, voids, or any inclusion in the material, the amplitude and shape of the signal received back to the transducer and results are normally interpreted and displayed on the screen and change in amplitude and shape of received signal are graphically represented for the inspected materials. During the inspection no change in amplitude or no change in shape of signals were observed on the displayed screen of the instrument, it shows no damage to the health and integrity of the surface and the components inspected are in good and satisfactory condition and are safe to operate at the flowing parameters. Results of MPI inspection are shown in table 7 below.

Table 5. UDF inspection results

Sr No	**Weld No**	**Results**
1	Weld No.1	Acceptable
2	Weld No.2	Acceptable

Weld joints were examined by ultrasonic flaw detector after proper calibration of the equipment, sub surface defects were the main targets in the weld joints. The echo or back wall echo in the ultrasonic flaw detector indicates such defects, however no such echo or back wall echo was observed during the inspection of equipment.

4.6 UT Gauging:

UT gauging was performed on all shells and nozzles. No major metal loss observed with comparison of design thickness. The thickness of Shell recorded was 24 mm, for Head A- Channel Head, Thickness is 24 mm, Thickness for Head B was 24 mm, Minimum thickness of A channel head 27.32 mm, minimum thickness for Head B 26,60 mm and minimum thickness for shell is 24.55 mm.

4.7 Ultrasonic thickness gauging:

Ultrasonic thickness gauging for the dish end, shell and nozzle conducted with the help of ultrasonic thickness meter. Results of thickness gauging are shown in table 6 below with minimum, maximum, and average thickness of each component. The lowest thickness is highlighted red for each component. All the readings are in millimeters (mm).

Table 6. Thickness gauging of dish end, Shell, and Nozzle

TML / CML #	Item Description	Min	Max	Avg
1	Location -1	26.83	27.80	27.32
2	Location – 2	24.10	24.68	24.39
3	S1	24.10	24.94	24.52
4	S2	24.23	24.97	24.60
5	S3	24.23	25.23	24.74
6	S4	24.25	25.23	24.74
7	S5	24.12	24.92	24.52
8	D-1	11.27	11.83	11.55
10	N-2	18.19	19.31	18.75
11	N-4	18.64	19.61	19.13

I. Minimum thickness observed during thickness gauging of the shell is 24.10 mm which is higher than the minimum required thickness of the shell and no potential threat observed.

II. The minimum thickness observed for the dish end of candidate equipment is 24.10 mm which is higher than the minimum required thickness no potential threat observed.

III. The minimum thickness for the nozzles noted is 18.19 mm which is higher than the minimum required thickness and no threat or significant metal loss observed.

IV. Location 1, location 2 , S1, S2, S3, S4, S5, D1 , N1 & N2 are marked on the Appendix – 1 Figure 34. for identification of thickness / conditions measuring locations.

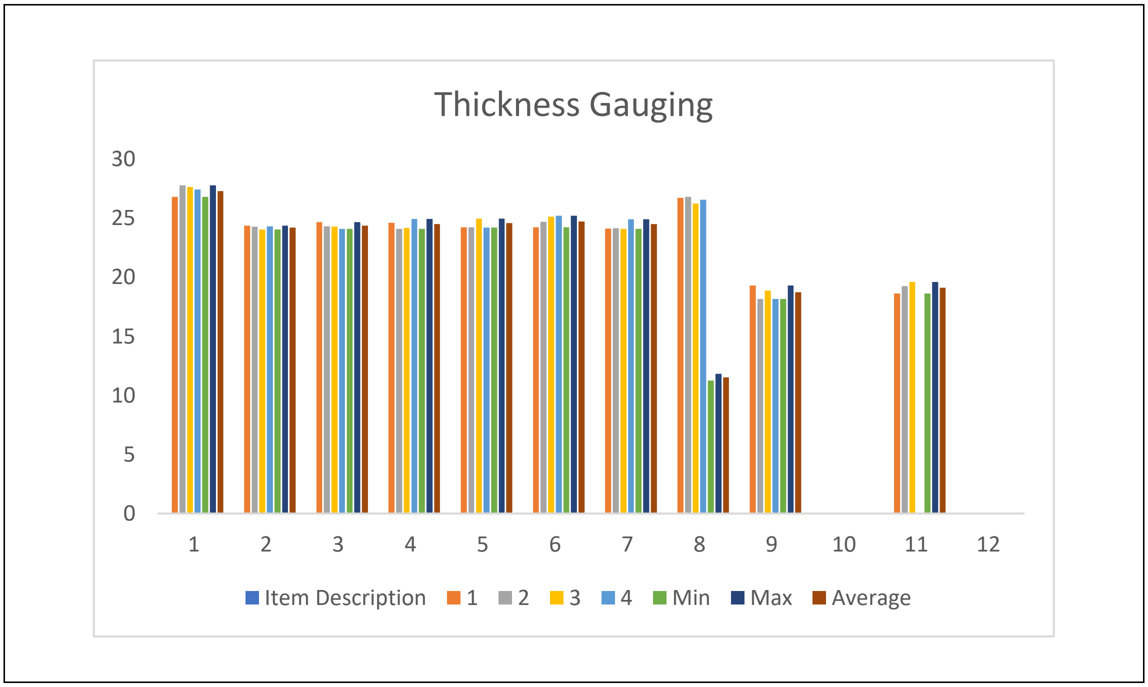

Figure 31. Thickness gauging results & comparison

4.8 Hardness Testing:

Hardness tests conducted by portable hardness tester are shown and the hardness values which are higher than 237 HB are highlighted against each component. All the values / readings are in HB.

Table 7. Hardness Testing of Base Metal, HAZ and weld

Sample # 01		**Sample # 02**	
Description	Average	Description	Average
Base Metal	238.67 [51]	Base Metal	311.67
HAZ	277.00 [51]	HAZ	256.33
Weld [52]	248.33 [51]	Weld	318.00
HAZ	259.50 [51]	HAZ	289.00
Sample # 03		**Sample # 04**	
Description	Average	Description	Average
Base Metal	155.00	Base Metal	362.33
HAZ	161.33	HAZ	313.67
Weld	167.33	Weld	309.00
HAZ	188.50	HAZ	300.00
Base Metal	163.25	Base Metal	286.50
Sample # 05			
Description	Average		
Base Metal	153.67		
HAZ	222.00		
Weld	176.33		
HAZ	219.00		
Base Metal	196.25		

The hardness of 05 sample was conducted by portable hardness tester after adopting proper procedure. The spot areas were Base metal, weld joints and HAZ areas. The HAZ area is one tenth the thickness of the weld.

After reviewing the values of hardness for sample # 02 & sample 04 found above the threshold values of the hardness. The threshold value of hardness is 237 HB. The higher values of samples #02 & 04 depict the material has not gone under proper heat treatment and high hardness values show a potential for increased brittleness. These spot areas may become more prone to cracking or fracturing under certain conditions.

4.9 On-Site metallography:

Results of metallography conducted at different sections / components are detailed below. The Metallography test for the spot area was conducted by 3 % Nital (it is a mixture of nitric acid & ethanol and is 2-3% concentrated nitric acid in ethanol) & at 200 X. [8]

The purpose of metallography by portable microscope as elaborated in figure no. was to investigate any changes in the microstructure of material. The material of construction is SA-517 Gr-70 which is normally in the form of hot rolled plate and used in pressure vessel as per ASME code. Material SA-516 Gr-70 have carbon contents 0.28, % Manganese 0.85-1.20%, Phosphorus (p) 0.035 %, Sulphur 0.035% and silicon (S) 0.15-0.40 %, ASME SA 516 Gr. 70 has tensile strength (Ksi) 70 - 90, Tensile strength (Mpa) 485 to 620, yield strength (Ksi) 38 and hardness is in the range 170 to 200 HB.

Metallography shows no change in microstructure because of any thermal stress, external stress and no anomalies seen, ferrite phase (White region) in a Pearlite matrix (dark regions). No major anomalies seen.

In the light of metallography by portable microscope conducted for different components, elbows where there is change in the direction of flow, the equipment is safe to operate at the flowing pressure and temperature. The test results are acceptable under the guidelines of ASME Section VIII div. which deals with the standard operating procedures and the tolerance limits of testing results.

Table 8. In-situ Metallography results

Sr#	Description	Results @ Magnification 200x
1	Elbow # 1	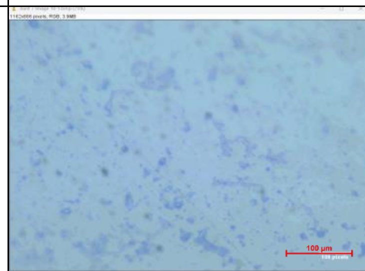 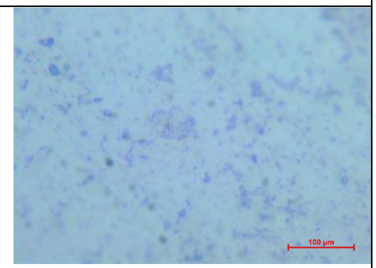
2	Elbow # 2	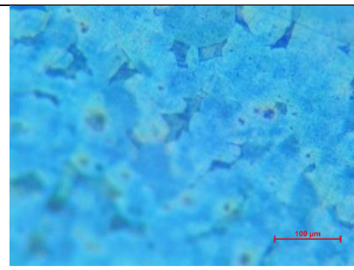 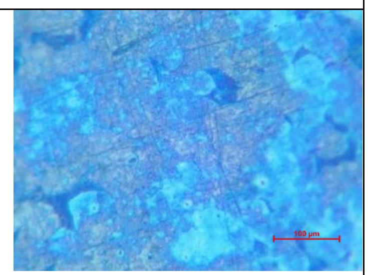
3	Elbow # 3	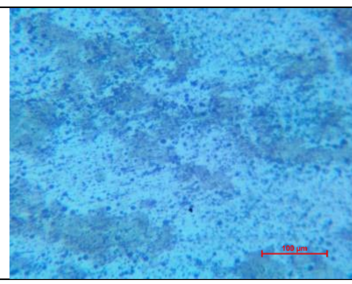 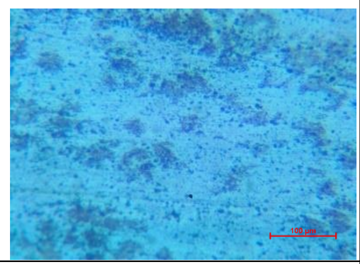
4	Elbow -4	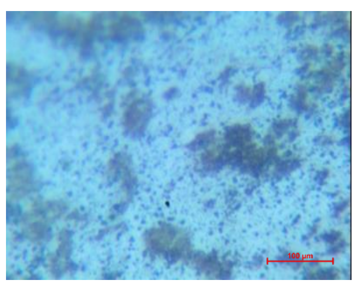 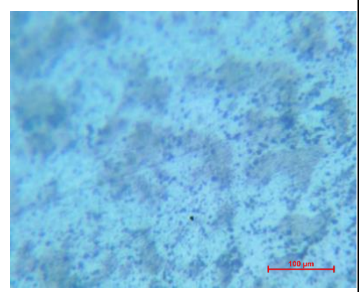
5	Elbow -5	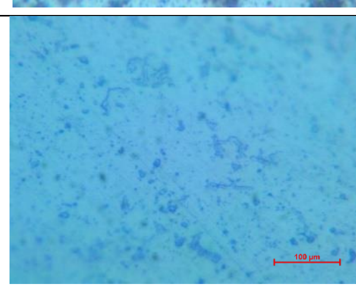 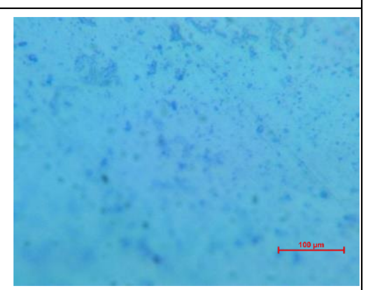

6	Elbow -6	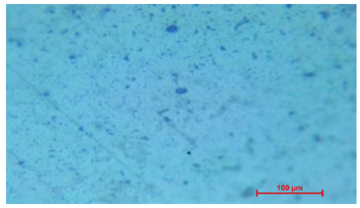 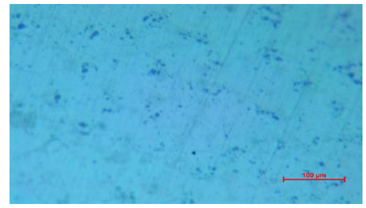
7	Elbow-7	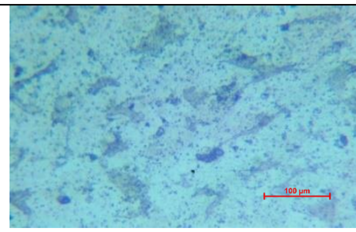 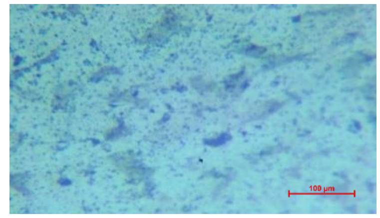

The above table shows the microstructure analysis of each part which has been inspected by portable metallographic technique.

After reviewing these microstructures and temperature conditions of the components, no anomalies have been observed and the microstructure consist of ferrite & perlite – matrix which show the material has gone through heat treatment process for relieving or residual stress.

4.10 Produced water Analysis Report:

Table 9. Produced water Analysis Report

Well Name	**H_2S (PPMs)**	**Pressure (psi)**	**Temperature (°F)**	**pH**	**Partial pressure (Psi)**
Well NO.1	4.5	1750	145.	6.6	0.7875
Well No.2	0.5	710	148.	6.6	0.04
Well No.3	1	1310	135.	6.6	0.131
Well No.4	9	500	141.	6.8	0.396
Well No.6	24	310	130.	6.8	2.184
Well No.7	0.5	960	124.	6.6	0.013
Well No.8	3	1030	153.	6.6	0.303
well No.9		1400	115.	6.8	
Re-Generation Gas Cooling & Heating System	**30**	**1250**	**145**	**6.7**	**3.75**

The above table is the produced water analysis along with PPMs of H_2S, temperature, pH, and partial pressure of different wells, coming from reservoir, partial pressure of each well is calculated to analyze the potential threat of H_2S with the yard stick of 0.05 Psi partial pressure.

After analyzing the partial pressure of H_2S in regeneration gas heating & cooling system, it is analyzed that the H_2S damage mechanism can occur as the conditions are very favorable for H_2S corrosion. [17]

4.11 Inspection finding summary:

Visual examinations and NDT activity were performed to assess metal loss rate and in-service damage. No major anomalies were found during inspection through Remote filed testing (RFT), dye penetration testing (DPT), Ultrasonic spot thickness survey (UT) and Magnetic particle testing / Inspection (MPI / PPT). [22]

4.11.1 Formulas for Key Parameter Calculations :

Calculations are done based on API-510 & ASME Sec VIII DIV 1 for corrosion rate, remaining life, MAWP, minimum required thickness. [53] Data used for calculation is taken from either name plate &/or General Engineering drawing/detailed drawing &/or historical data. [54]

1) Minimum Required Thickness Head(A), $\mathrm{T} = \frac{(\mathrm{PXD})}{2\times\mathrm{S}\times\mathrm{E}-0.2\times\mathrm{P}}$
2) Minimum Required Thickness Head (A), $\mathrm{Tr} = \frac{(\mathrm{PXD})}{\mathrm{T}(2\times\mathrm{S}\times\mathrm{E}-0.2\times\mathrm{P}}$
   (ASME Sec, VIII Div 1 UG:32)
3) Minimum Required Thickness cylindrical shell, $\mathrm{T} = \frac{(\mathrm{P}\times\mathrm{R})}{(\mathrm{S}\times\mathrm{E}-0.6\times\mathrm{P}}$
4) Minimum Required Thickness Head (B), $\mathrm{T} = \frac{(\mathrm{PXD})}{(\mathrm{S}\times\mathrm{E}-0.6\times\mathrm{P}}$
5) (ASME Sec VIII Div 1 UG:32)
6) Corrosion Rate Short Term (ST), (shell)

$$\mathrm{CRST} = \frac{\mathrm{Tprevious}-\mathrm{Tactual}}{\mathrm{time}\ b.w\ previous\ and\ current\ inspection}$$

7) $$\text{Remaining life} = \frac{\text{Tactual}-\text{T required}}{\text{corrosion rate}}$$

8) Maximum allowable working pressure, (MAWP), $\mathrm{P} = \frac{(\mathrm{TS}\times\mathrm{t}\times\mathrm{E})}{(\mathrm{R}\times\mathrm{SF})}$

TS is Tensile strength of metal, t is the thickness, E is efficiency, R is the radius, SF is safety factor. P is pressure, D is inside diameter, S is allowable stress value, E is joint efficiency.

4.11.2 Calculation of Key Parameters:

Calculation of remaining life, maximum allowable working operating pressure, corrosion allowance, remaining life, and next inspection internal for regeneration gas sub cooler was conducted under the ASME Sec VIII Div I UG [47]) and the API- 510 [9]. Table 1 shows the calculation.

Table 10. Calculation for corrosion rate, remaining life, maximum allowable working, and operating pressure

Sr#	Description	Result
1	Minimum Required Thickness Head (A, in mm), (ASME Sec, VIII Div 1 UG:32 [53]) and from above mentioned formula 1	15.71
2	Minimum Required Thickness cylindrical shell in mm, (ASME Sec, VIII Div 1 UG:32) and from above mentioned formula- 1	17.54
3	Corrosion Rate Short Term (ST, in mm/year), **(shell)** and from above mentioned formula – 8	0.47
4	Corrosion Rate Short Term (ST in mm/year), **(Head)** and from above mentioned formula- 8	0.48
5	Remaining life (year), Head A and from above mentioned formula- 9	24.18
6	Remaining life (year), shell and from above mentioned formula - 9	14.91
7	Maximum allowable working pressure (Psig), Head A from above mentioned formula- 10	2163.60
8	Maximum allowable working pressure (Psig), Shell, from above mentioned formula- 10	1721.63
9	Maximum allowable working pressure (Psig), Head B, from above mentioned formula- 10	1954.50

Short term corrosion rate calculated is calculated based on previous and actual thickness of the shell and tubes and the corrosion rate calculated is 0.47 mm / year or 18.50 mpy. According to NACE

I. Negligible Corrosion Rate: Corrosion rate less than 0.1 mm/year (4 mils/year) [35]
II. Low Corrosion Rate: Corrosion rate between 0.1 mm/year (4 mils/year) and 0.5 mm/year (20 mils/year)
III. Moderate Corrosion Rate: Corrosion rate between 0.5 mm/year (20 mils/year) and 2.5 mm/year (100 mils/year)
IV. High Corrosion Rate: Corrosion rate between 2.5 mm/year (100 mils/year) and 10 mm/year (400 mils/year)
V. Very High Corrosion Rate: Corrosion rate exceeding 10 mm/year (400 mils/year)

However, the corrosion rate calculated for shell and head is in the category of low, also the minimum required thickness and allowable maximum operating and work pressure is within the safe limits. Therefore, the equipment is safe to operate at the flowing parameters. [35]

5 Conclusions

1. Short term Corrosion rate calculated from previous and actual thickness is 0.45 mm/ year (18.5 MPY) which is exceptionally low corrosion rate, the remaining life for head is 24.18 14.91 years.. Whereas the corrosion rate for head is 0.48 mm / year (18.89 MPY) and the remaining life calculated is 14.91 years. Therefore, it is concluded that the equipment is safe to operate.
2. Comprehensive visual inspections (internal and external), as well as nondestructive testing techniques including eddy current (RFT), dye penetrant testing (DPT), magnetic particle inspection (MPI), ultrasonic flaw detection (UFD), ultrasonic thickness gauging (UTG), hardness testing, and in-situ metallography, were conducted. Lab analysis results of the gas composition showed the absence of surface, near surface, and sub-surface defects. The inspection reports suggest the presence of an Iron sulfide layer on the equipment's surface, hypothesized to function as a protective barrier. This layer is assumed to remain stable up to a concentration of 50 parts per million (PPMs), as indicated by the comprehensive inspection findings.".
3. During the inspection of the tubes, metal loss was observed in two tubes. The Remote Field Testing (RFT) results of the equipment's tubes revealed that certain tubes were clogged. To resolve this issue, water jetting was performed to clean the affected tubes. Additionally, a batch treatment of corrosion inhibitor was applied to prevent further corrosion. In areas where metal loss was observed, appropriate materials were used to plug those tubes and prevent any potential leakage or additional metal loss.
4. The measured thickness of the shell and head during the current inspection is 24.55 mm for the shell and 16.95 mm for Head B. For Head A, the measured thickness is 15.71 mm. These measurements exceed the minimum required thickness of 17.54 mm for the shell and 26.60 mm for Head B, and 27.32 mm for Head A.
5. Based on the calculations, the Maximum Allowable Working Pressure (MAWP) for the Inlet Gas Regeneration Cooling & Heating system installed at the oil field is determined to be 1721 psig for the shell side, 1954 psig for Head B, and 2163 psig for

Head A. These values are higher than the operating pressures, showing that the equipment is safe to operate within the current operating parameters.

6. Hardness values for sample #02 and sample 04 show above the threshold value of hardness, the said areas are susceptible to cracking and fracture. The increase in hardness depicts improper heat treatment of the part during fabrication / welding procedure.
7. The equipment Regeneration gas cooling and heating system is safe to operate at the current operating parameters.

6 Recommendation against H_2S corrosion mitigations:

Based on the above inspections and their results, following are the recommendations

1. H_2S scavenger to be installed to control the concentration of H_2S (below 50 PPMs and below 0.05 Psi partial pressure). [10]
2. Appropriate Corrosion inhibitor to be injected uninterruptedly and continuously to neutralize the electrolyte and injection of the chemicals be optimized through residual testing and the care should be taken to select the injection point.
3. Periodic hardness testing to be conducted to check the hardness level through available portable hardness meter. TMLS / CMLs selections should be based on the weld joints, heat affected zones (HAZs) and areas where hardness reached above 237 HB value, special attention to be avoid any rupture / damage to the surface. [6]
4. Pre-hardened coupons to be installed to check the impact of H_2S corrosion and the coupons to be retrieved not before 90 days from the date of installation of these coupons. [10]
5. The installed coupons to be checked for any surface cracks through available inspection techniques.
6. To mitigate the high hardness in the components of regeneration gas cooling and heating system, proper heat treatment process be applied to reduce the stresses reported in elbows of the equipment. [6]
7. Surface analysis through surface inspection defects to be conducted through dye penetration tests, Hardness testing through portable hardness tester and metallography to observer any change in metallurgy / structure of the materials and other available sub – surface inspection techniques to use to check the integrity and health of the material.
8. Continuous monitoring of fluid to check the concentration of H_2S and pH to be checked on periodical basis.
9. Produced water sampling was conducted to check the iron and manganese count and pH of the fluid.

APPENDIX- I

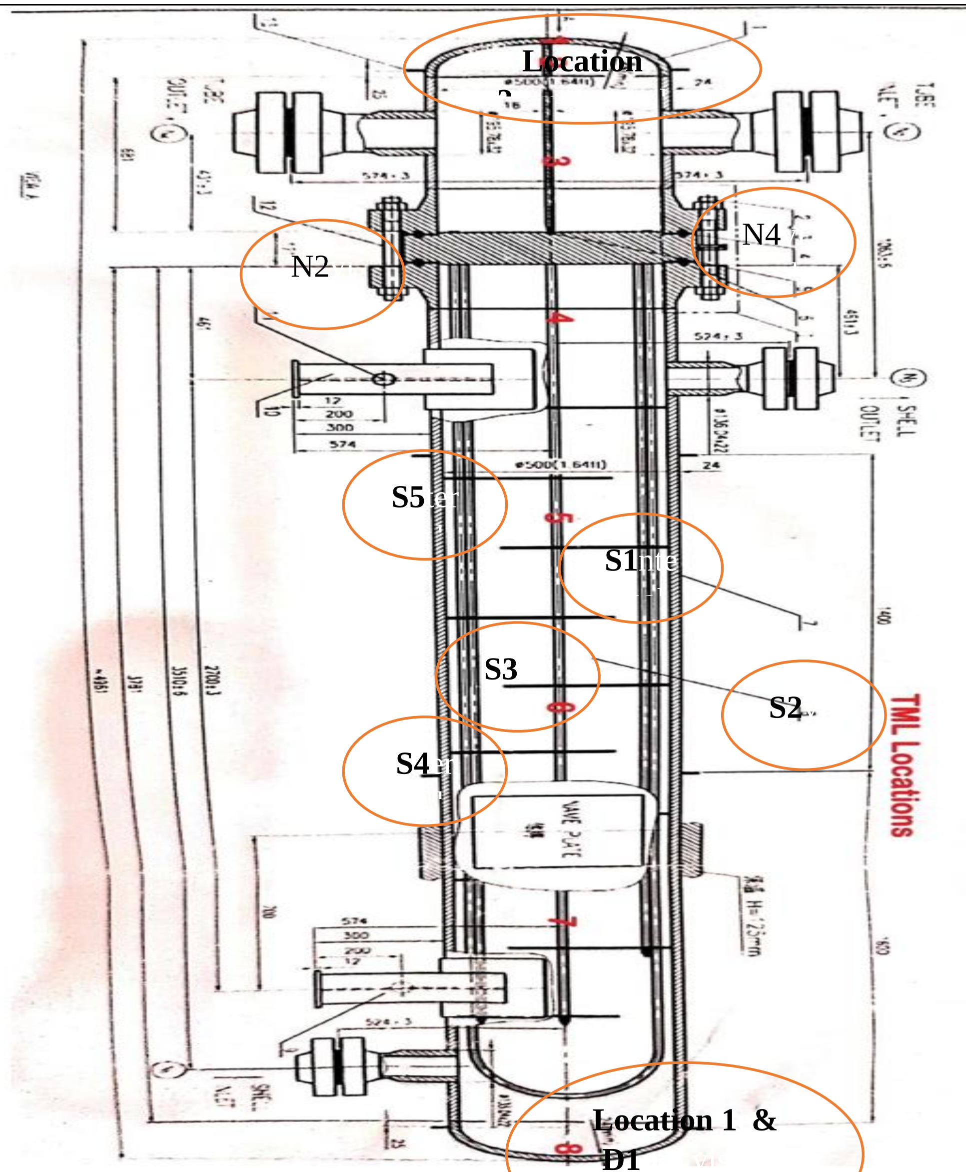

Figure 32. Sketch for regeneration gas fooling and heating system

APPENDIX- II

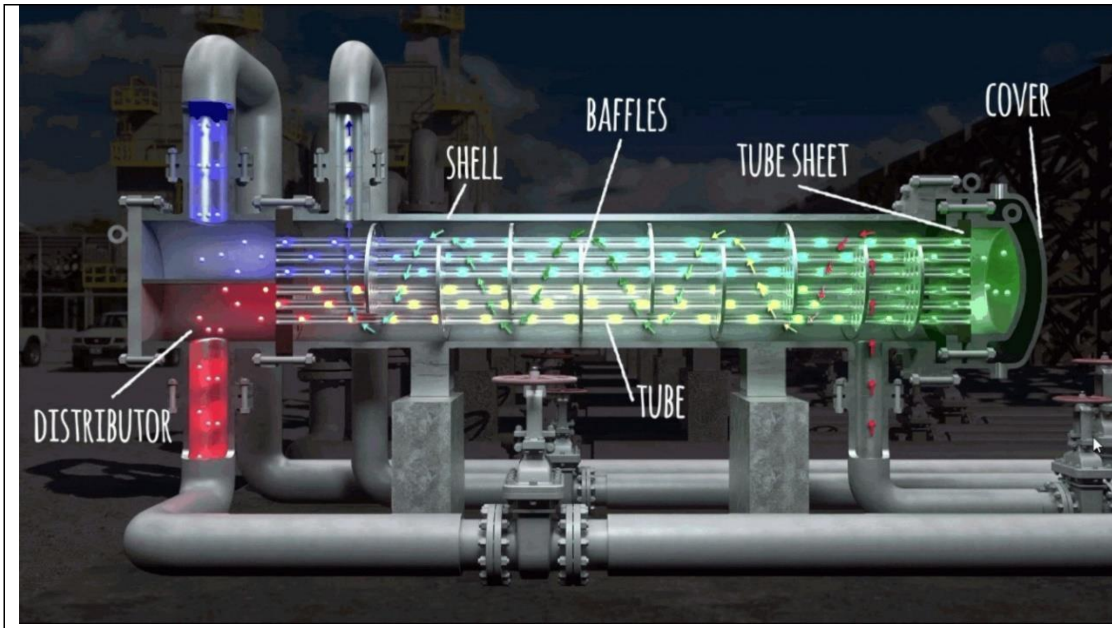

Figure 33. 3D overview of regeneration gas heating and cooling system

References

[1]. Guidelines For Quantitative Risk Assessment, C. 18e, Editor. June (2014).

[2]. Zhihong Wang, C.Y., Lin Zhu, Corrosion Analysis And Inhibition Studies In The Process Of Natural Gas Wet Desulfurization. Elsevier, April (2014).

[3]. (Api), A.P.I., In-Service Inspection, Rating, Repair, And Alteration Of Pressure Vessels In Api 510 Edition-May 2014, Addendum (2018).

[4]. Engineer, A.S..M.E, Inspection Of Pressure Vessel, In Asme Section Viii Div. 1. (2015).

[5]. Insitute, A.P., Risk Based Inspection, In Api 581. (2016).

[6]. Institue, A.P., Welding Of Pipelines And Related Facilities, In Api Standard 1104. September (2018).

[7]. Engineer, N.A.F.C., General Principles For Selection Of Cracking-Resistant Materials, In Nace Mr0175 / Iso 15156-1 (2016).

[8]. Insitute, A.P., Inspection Practice For Pressure Vessel Fourth In Api 572 Edition-December (2016).

[9]. Insitute, A.P., Pressure Vessel Inspection Code:In-Service Inspection, Rating, Repair, And Alteration, In Down Stream Segment. June (2006).

[10]. (Nace), N.A.C.E., Stress Corrosion Cracking (Scc) Direct Assessment Methodology, In Sp0204. (2015).

[11]. Rafael Nardon Ferraresi1, V.C.D.C., Gabriel Cicelini1, Weslley Carlos Dias Da Silva2, Ruham Pablo Reis1 蒡, Valtair Antônio Ferraresi1, Analysis Of Non-Destructive Tests For Inspection Of Tubes From Shell-And-Tube Heat Exchangers: Remote Field (Rft) Versus Internal Rotary Inspection System (Iris). Soldagem & Inspecao, May (2021).

[12]. Roberge, P.R., Corrosion Engineering Principles And Practice. (2008): Mcgraw-Hill.

[13]. Insitute, A.P., Damage Mechanisms Affecting Fixed Equipment In The Refining Industry, In Ansi / Api Recommended Practice 571. March (2020).

[14]. Ren, L., Et Al., Simulation Of The Relationship Between Calcium Carbonate Fouling And Corrosion Of Iron Surface. (2019). **582**: P. 123882.

[15]. Demadis, K.D.J.C.H.E. And E.T.F.T.P. Industries, Combating Heat Exchanger Fouling And Corrosion Phenomena In Process Waters. (2003): P. 483-490.

[16]. Obuka, N.S.P., Review Of Corrosion Kinetics And Thermodynamics Of Co2 And H2s Corrosion Effects And Associated Rediction/Evaluation On Oil And Gas Pipeline System. International Journal Of Scientific & Technology Research, May (2012). **Volume 1,**.

[17]. Enginner, N.A.F.C., Materials For Use In H2s-Containing Environments In Oil And Gas Production December 2005, In Nace Mr0175 / Iso15156. December (2005).

[18]. Yadla, S.V., A Review On Corrosion Of Metals And Protection. International Journal Of Engineering Science & Advanced Technology, May-Jun (2012). **Volume-2, Issue-3, 637 – 644**.

[19]. Harsimran, S., Overview Of Corrosion And Its Control: A Critical Review. (2021). **Pes**.

[20]. A. Davoodi A, M. Pakshir B, M. Babaiee B, G.R. Ebrahimi, A Comparative H2s Corrosion Study Of 304l And 316l Stainless Steels In Acidic Media. Elsevier, October (2010).

[21]. Jancler Adriano Pereira Nicacio 1, V.D.F.C.L., Alexandre Queiroz Bracarense, Failure Analysis In Heat Exchanger Tubes From The Top System Of The Regeneration Tower Of The Hydrotreatment Unit In An Oil Refinery: A Case Study. Revistamateria, (2021). **V.26**.

[22]. Insitute, A.S..M.E.A.P., Fitness-For-Service, In Api 579-1/Asme Ffs-1. (2016).

[23]. Saibo Shea, Y.C., Yunzeheabc, Zhongji Zhouc, Xiangzoua, Optimal Design Of Remote Field Eddy Current Testing Probe For Ferromagnetic Pipeline Inspection. Elsevier, (2021). **168**.

[24]. Insitute, A.P., Piping Inspection Code: In-Service Inspection, Rating, Repair, And Alteration Of Piping Systems. February (2016).

[25]. Mohammed, M.F.S.A.S.F.T., Failure Analysis Of Heat Exchanger Using Internal Rotary Inspection System (Iris). Springer, 2021.

[26]. Yuxin Chen, S.Z., Influence Of H2s Interaction With Prestrain On The Mechanical Properties Of High-Strength X80 Steel. Elsevier, Janurary (2016).

[27]. Xingjiang, Z.Q.S.Y.R.S.L.H.Z., Corrosion Failure Analysis On Heat Exchanger Pipes. Springer, November (2016).

[28]. (Api), A.P.I., Piping Inspection Code: In-Service Inspection, Rating, Repair, And Alteration Of Piping Systems, In Api 570. (2015).

[29]. Pengyan Wang A, J.W.A., Shuqi Zheng A,*, Yameng Qi B, Maoxian Xiong A, Yanjun Zheng, Effect Of H2s/Co2 Partial Pressure Ratio Onthe Tensile Properties Of X80 Pipeline Steel. Elsevier, May (2015).

[30]. H. Panahia, A.E., ⁎, M.A. Golozara, A. Ashrafi Lalehb, M. Aryanpurb, M. Mazareib, Failure Analysis Of Type 304 Stainless Steel Amine Exchanger Sheets In A Gas Sweetening Plant. Elsevier, August (2017).

[31]. Sikes, M.A., Et Al. H2s Challenges Presented To Esp Systems. In Spe Middle East Oil And Gas Show And Conference. (2011). Spe.

[32]. Dong, B., Investigation On Mechanical Properties And Corrosion Behavior Of Rubber For Packer In Co2-H2s Gas Well Elsevier, March (2021).

[33]. Monnota, M., Sulfide Stress Corrosion Study Of A Super Martensitic Stainless Steel In H2s Sour Environments: Metallic Sulfides Formation And Hydrogen Embrittlement Elsevier, October (2016).

[34]. Zhao, M.-C., Investigation On The H2s-Resistant Behaviors Of Acicular Ferrite And Ultrafine Ferrite. Elsevier, Janurary (2002).

[35]. (Nace), N.A.F.C.E., Preparation, Installation, Analysis, And Interpretation Of Corrosion Coupons In Oilfield Operations, In Nace Standard Rp0775-2005. (2005).

[36]. Y. P. Asmara*, J., J. Jaafar, K. Azuar, J.P. Siregar, T. Kurniawan, Effects Pre-Strain Of Carbon Steel On Stress-Strain Diagram In Co2 Environment With The

Presence Of H2s. International Journal Of Material Science Innovations (Ijmsi), June (2014).

[37]. Z.Y. Liu, X.Z.W., R.K. Liu, C.W. Du, And X.G. Li, Electrochemical And Sulfide Stress Corrosion Cracking Behaviors Of Tubing Steels In A H_2s/Co_2 Annular Environment. Springer, (2013). **Volume 23(4**.

[38]. W. Yan, J.D., P. Zhu, Investigation Of Ph2s Influence On 3% Cr Tubingsteel Corrosion Behaviours In Co2–H2s–Cl−Environment. Taylor & Francis, (2015).

[39]. Ming-Chun Zhao, Role Of Microstructure On Sulfide Stress Cracking Of Oil And Gas Pipeline Steels. Metallurgical And Materials Transactions A, May (2003). **34a**.

[40]. Anijdan, S.H.M., Sensitivity To Hydrogen Induced Cracking, And Corrosion Performance Of An Api X65 Pipeline Steel In H2s Containing Environment: Influence Of Heat Treatment And Its Subsequent Microstructural Changes. Elsevier, July (2021).

[41]. Caratozzolo, V., Et Al., A Generalized Equipment Vulnerability Model For The Quantitative Risk Assessment Of Horizontal Vessels Involved In Natech Scenarios Triggered By Floods. 2022. **223**: P. 108504.

[42]. Lu, Y., V. Lagad, And R. Alvarez. Case Studies Of Corrosion Failures Due To Poor Design And Non-Optimized Materials Selection. In Nace Corrosion. (2019). Nace.

[43]. Prueter, P.E., A Guide To Corrosion Under Insulation Management. (2022): P. 4.

[44]. Cao, Q., Et Al., A Review Of Corrosion Under Insulation: A Critical Issue In The Oil And Gas Industry. (2022). **12**(4): P. 561.

[45]. Liu, C., Investigation On The Corrosion Behavior Of Ni-Cr-Mo-W-Xsi Laser Cladding Coating In H2s Corrosion Environment. Elsevier, November (2021).

[46]. K.-J. Metzner, U.W., European Therfat Project—Thermal Fatigue Evaluation Of Piping System “Tee”-Connections. Elsevier, (2004).

[47]. (Asme), A.S.F.M.E., Asme Sec V Nondestructive Examination In Nondestructive Examination. 2015.

[48]. (Asme), A.S.O.M.E., Ansi/Asme B31.1 Power Piping, In Chemical & Oil Refineries. (2002).

[49]. Materials, A.S.F.T.O., Standard Test Method For Brinell Hardness Of Metallic Materials, In Astm E10-15. 2014.

[50]. Saibosheayifangchenayunzeheabczhongjizhoucxiangzoua, Optimal Design Of Remote Field Eddy Current Testing Probe For Ferromagnetic Pipeline Inspection. Elsevier, 15 January (2021). **168**.

[51]. Nace, Nace Rp 0175. (2005).

[52]. 1104, A.S., Welding Of Pipelines And Related Facilities(2018).

[53]. Engineer, A.S.F.M., Manual For Determining The Remaining Strength Of Corroded Pipelines, In Asme B31g-2012. (2012).

[54]. Asme, B31g, Remaining Life. (2012).